Geophys. J. Int. (2003) **153,** 111–132

Long-term elasticity in the continental lithosphere; modelling the Aden Ridge propagation and the Anatolian extrusion process

Aurélia Hubert-Ferrari,[1] Geoffrey King,[2] Isabelle Manighetti,[2] Rolando Armijo,[2] Bertrand Meyer[2] and Paul Tapponnier[2]

[1] *Geosciences Department, Princeton University, Princeton,* NJ 08544, *USA*
[2] *Laboratoire de Tectonique, IPGP,* 4 *Place Jussieu, Paris,* 75252, *Cedex* 05, *France*

Accepted 2002 October 16. Received 2002 October 9; in original form 2002 January 14

SUMMARY

The evolution of the Gulf of Aden and the Anatolian Fault systems are modelled using the principles of elastic fracture mechanics usually applied to smaller scale cracks or faults. The lithosphere is treated as a plate, and simple boundary conditions are applied that correspond to the known plate boundary geometry and slip vectors. The models provide a simple explanation for many observed geological features. For the Gulf of Aden the model predicts why the ridge propagated from east to west from the Owen Fracture Zone towards the Afar and the overall form of its path. The smaller en echelon offsets can be explained by upward propagation from the initially created mantle dyke while the larger ones may be attributed to the propagating rupture interacting with pre-existing structures. For Anatolia the modelling suggests that the East Anatolian Fault was created before the North Anatolian Fault could form. Once both faults were formed however, activity could switch between them. The time scales over which this should take place are not known, but evidence for switching can be found in the historical seismicity.

For Aden and Anatolia pre-existing structures or inhomogeneous stress fields left from earlier orogenic events have modified the processes of propagation and without an understanding of the existence of such features the propagation processes cannot be fully understood. Furthermore a propagating fault can extend into an active region where it would not have initiated. The North Anatolian Fault encountered slow but active extension when it entered the Aegean about 5 Ma and the stress field associated with the extending fault has progressively modified Aegean extension. In the central Aegean activity has been reduced while to the north-west on features such as the Gulfs of Evvia and Corinth activity has been increased.

The field observation that major structures propagate and the success of simple elastic models suggest that the continental crust behaves in an elastic-brittle or elastic-plastic fashion even though laboratory tests may be interpreted to suggest viscous behaviour. There are major problems in scaling from the behaviour of small homogeneous samples to the large heterogeneous mantle and large-scale observations should be treated more seriously than extrapolations of the behaviour of laboratory experiments over many orders of magnitude in space and time. The retention of long-term elasticity and localised failure suggests a similar gross rheology for the oceanic and continental lithospheres. Even though it is incorrect to attribute differences in behaviour to the former being rigid (i.e. elastic) and the latter viscous, oceanic and continental lithosphere behave in different ways. Unlike oceanic crust, continental crust is buoyant and cannot be simply created or destroyed. The process of thickening or thinning works against gravity preventing large displacements on extensional or contractional features in the upper mantle. The equivalents of ridge or subduction systems are suppressed before they can accommodate large displacements and activity must shift elsewhere. On the other hand, strike-slip boundaries and extrusion processes are favoured.

Key words: Anatolian Fault, continental deformation, fault propagation, Gulf of Aden.

INTRODUCTION

It is now generally accepted that ocean ridges are created by a process of propagation (MacDonald *et al.* 1991) and can be modelled using modifications of elastic fracture mechanics (Knott 1973; Lawn & Wilshaw 1975; Morgan & Parmentier 1985). Similar concepts have also been adopted to describe the evolution of faults of moderate scales (e.g. Rudnicki 1980; Cowie & Scholz 1992a,b; Dawers *et al.* 1993; Bürgmann *et al.* 1994; Peacock & Sanderson 1996; Martel 1997; Martel 1999; Gupta & Scholz 1998). Elastic fracture mechanics can be applied where deformation is localised and the surrounding material can be treated as being elastic. While this has been accepted for the oceanic lithosphere and for the seismogenic crust of the continents, many authors have suggested that the effective rheology of the continental lithosphere is viscous (e.g. England & McKenzie 1982; Vilotte *et al.* 1982; Houseman & England 1986, 1989; England & Jackson 1989). While numerous models with a viscous or more complex rheology have been offered (e.g. Bird 1991; Klein *et al.* 1997; Cianetti *et al.* 1997; Lundgren *et al.* 1998; Meijer & Wortel 1997; Martinod *et al.* 2000; Cloetingh *et al.* 1999), none have suggested that a simple modification of elastic fracture mechanics can be applied to deformation of the continental lithosphere at a large scale. However, increasing evidence suggests that major faults cutting the lithosphere have evolved by propagation and that continental deformation can be highly localised (e.g. Armijo *et al.* 1996; Peltzer *et al.* 1982; Tapponnier *et al.* 1982; Peltzer & Tapponnier 1988; Briais *et al.* 1993; Leloup *et al.* 1995; Peltzer & Saucier 1996; Meyer *et al.* 1998; Ebinger *et al.* 2000; Murphy *et al.* 2000). Deformation between these fault zones seems to be small, suggesting that elasticity can be a useful approximation to the behaviour of the continental lithosphere. Laboratory evidence (e.g. Brace & Kohlstedt 1980) used to suggest that lower crust and upper-mantle rocks deform in a viscous fashion can be misleading. Changing the boundary conditions from those used in sample tests can alter dramatically the behaviour of some materials. McClintock (1971) emphasizes this in a landmark paper dealing with engineering materials, which starts with the following sentences 'Why discuss ductile fracture in a book on brittle fracture? Because a ductile material can sometimes lead to a brittle structure; i.e. a structure with a nearly linear elastic-load deformation curve to fracture.'

Nonetheless, continental lithosphere is different from materials to which fracture mechanics is normally applied. Fracture toughness is not a material property but scales with fault size (Cowie & Scholz 1992a,b). Continental lithosphere contains defects (or inhomogeneities) at all scales. Furthermore the boundary conditions applied to any region are complex and very different from the conditions in which samples can be tested. The presence of large defects prevents the path of propagating ruptures from being strictly predictable since a propagating rupture can be deflected during its progress. The course that a fracture takes depends on the location of pre-existing features, some of which can be recognised only retrospectively. This means that the evolution of continental boundaries, like the evolution of Life can only be understood retrospectively.

Although the predictive power of modelling in such media is necessarily limited, simple questions can be posed and simple conclusions drawn. Can the known plate boundary conditions account for the observed evolution of a propagating boundary? Is the observed direction of propagation consistent with that suggested by modelling? Can observed variations of propagation directions be explained by pre-existing structures? If modelling of this sort is successful it has important implications. It suggests that while the lithosphere need not be elasto-plastic or elasto-brittle at all depths, in so far as such fracture mechanics models work at the large scale, the gross behaviour of the continental lithosphere *is* elasto-plastic and develops structures that appear to be brittle.

This paper first describes two structures that have been shown to have evolved by propagation, the Gulf of Aden Ridge and the Anatolian Fault System. The former provides an example of an ocean ridge propagating into well-established continental lithosphere while the two Anatolian faults illustrate the effects of continental collision in the creation of major strike-slip faults. The assumptions behind the modelling techniques are then described and illustrated with simple models. Finally the broader implications are discussed. It is noted that the geological evolution of fault systems such as those in Anatolia require stress systems that must evolve with time. Little data exists to determine the time scales of such evolution, but evidence for temporal changes of seismicity suggests that variations over periods of hundreds of years may be involved. A modification of simple fracture mechanics models also suggest why continental strike-slip faults have greater longevity than reverse or normal faults. Dip slip features create topography, which in turn creates gravitational stresses resisting further motion. Although extensional fault systems sometimes evolve to become ocean ridges, in general dip slip features have a limited life before deformation must move to new structures elsewhere.

THE REGIONS STUDIED

The boundaries we discuss are related to the interaction between the Eurasian, African and Arabian plates (Fig. 1). The pole of rotation between Africa and Eurasia lies in the eastern Atlantic (21°N, −21.6°E, De Mets *et al.* 1990) and gives an Africa to Eurasia converge rate of about 10 mm yr^{-1} at the longitude of Arabia. The Arabian Plate moves with respect to Africa about a pole located in the Eastern Mediterranean (32.8°N, 22.6°E, Garfunkel 1981) giving an opening rate of about 20 mm yr^{-1}. for the Gulf of Aden (Garfunkel 1981; Joffe & Garfunkel 1987). The regions studied in this paper are located on the southern and northern boundaries of the Arabian Plate (Fig. 1).

The Arabian Plate is bounded in the south and southwest by divergent boundaries forming the Gulf of Aden and the Red Sea. The former now has the characteristics of an ocean ridge (with magnetic anomalies and transform offsets). Elsewhere these boundaries are apparently transitional between continental extension and the onset of ocean spreading. To the east, along the Owen Fracture Zone, strike-slip motion occurs between the Arabian and Indian plates. The rate and history of this motion is well determined from the evolution of the Carlsberg ridge. To the west, predominantly strike-slip motion occurs along the left-lateral Dead Sea fault. To the north, the Arabian-Eurasian plate boundary is associated with contraction, at a rate of about 30 mm yr^{-1}. As a result of the contraction, the high mountain ranges of the Zagros and the Caucasus have been created. To the west, the Anatolian Block has been extruded away from the collision zone toward the Aegean Subduction System.

The Gulf of Aden: ridge propagation from oceanic to continental lithosphere

Prior to the opening of the Gulf of Aden, Arabia was attached to Africa. The Red Sea, which was much narrower, formed a continuation of the East African rift (e.g. Manighetti *et al.* 1997). Figs 1and 2

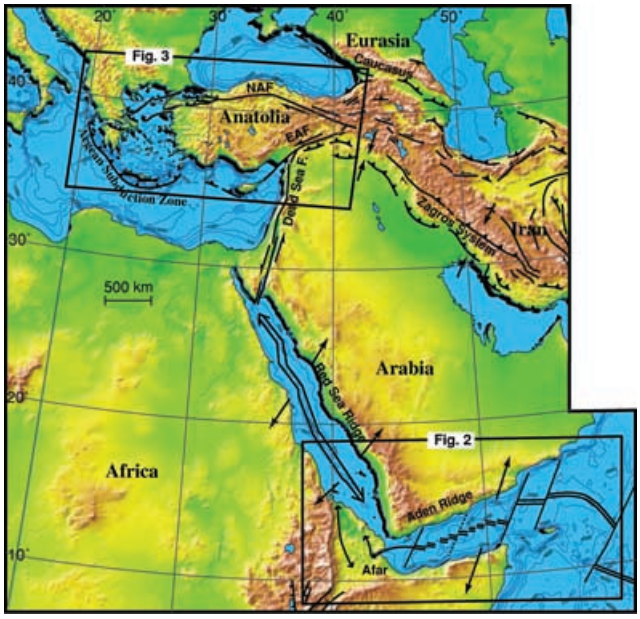

Figure 1. The geodynamic setting of the study area. The Arabian plate is moving northward relative to Africa opening the Gulf of Aden and the Red Sea. To the North it collides with Eurasia creating the mountain ranges of the Zagros and the Caucasus. In the Northeast, the Anatolian block is extruded westward between the East and North Anatolian strike-slip faults (EAF and NAF).

show the form of the present active spreading zone with magnetic anomalies being identifiable between the Owen Fracture Zone and the Shukra El Sheik Transform.

The section between the Socotra Transform and the Shukra El Sheik Transform exhibits en echelon offsets with ridge segments connected by transform faults. To the east and west of this zone, the spreading systems have smoother arcuate forms with perhaps small scale segmentation in the east and small offset basins in the west (Audin 1999). For the Eastern Sheba Ridge, the magnetic anomalies are also curved and unlike the segmented parts of the ridge, the sea floor morphology shows no evidence for earlier segmentation. The change from a smoothly curved rift to the segmented rift at the Socotra Transform occurs where the original rift started to cut continental lithosphere. To the west of the Alula Fartak Transform, the Central Ridge cuts across the Arabian-Somali Craton. In the west the smoother form reappears near to the outer limit of lithosphere modified by the Afar plume.

The rift has propagated 1500 km from east to west; the oceanic crust tapers to the west and magnetic anomalies also young westwards (Tisseau 1978; Courtillot *et al.* 1980; Cochran 1981) giving the overall impression of a propagating lithospheric crack (Courtillot *et al.* 1980; Cochran 1981). Manighetti *et al.* (1997) (from which this section is summarized) identify further details of the propagation processes. The ridge initiated about 30 Ma and propagated at average rates greater than 10 cm yr^{-1}. The propagation was arrested a number of times, for about 3 Ma at the Error-Sharbitat kink zone (too small to be visible at the scale of Fig. 2), about 4 Ma at the Alula

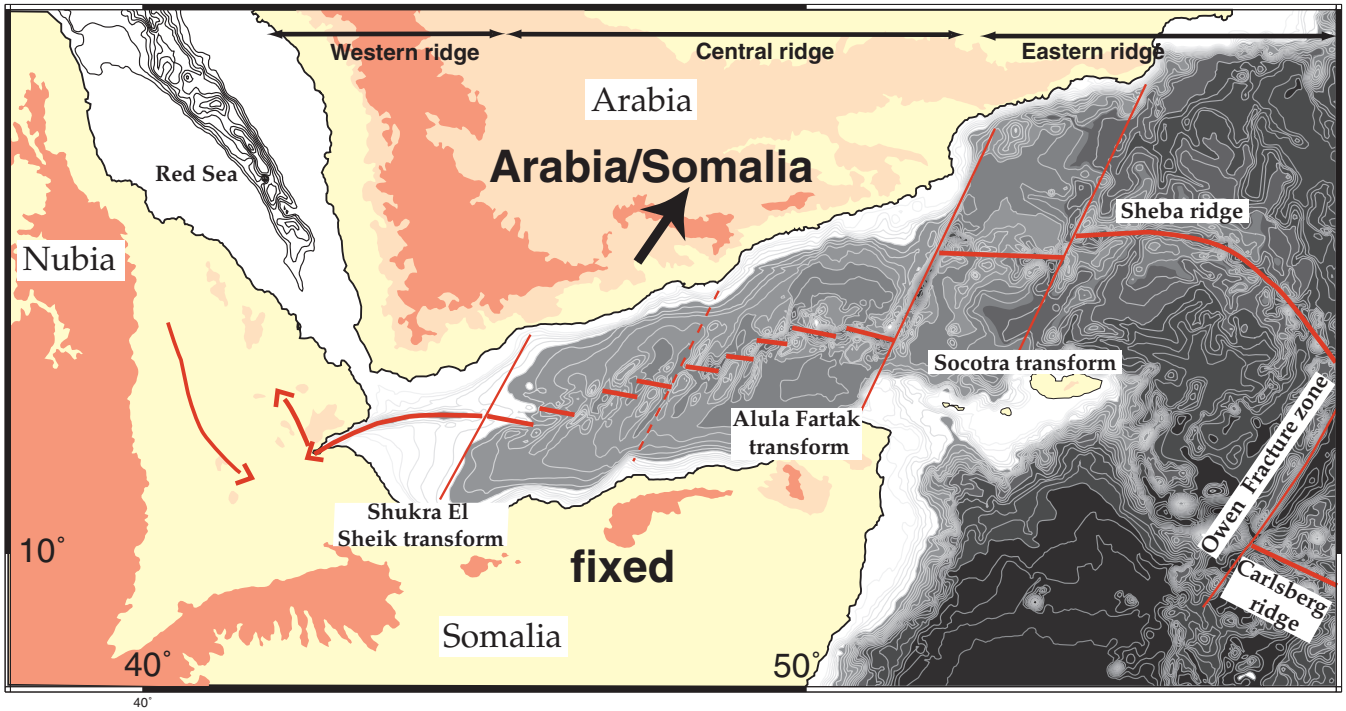

Figure 2. Characteristics of the Aden ridge (bathymetric contours every 200 m). In the east the ridge veers smoothly (at the scale of the figure) after leaving the Owen Fracture zone at an angle close to 45°. Opening is oblique. Between the Socotra transform and the Shukra El Sheik transform, the ridge is segmented in a form typical of ocean ridges. Transform faults are parallel to the slip vector and opening segments are perpendicular to the slip vector. At the western end, the valley along which opening is concentrated again adopts a smooth arcuate form.

Fartak and 13 Ma at the Shukra El Sheik. The arrests were apparently caused by temporary barriers to fracture propagation across pre-existing structures parallel to the old African-Arabian coast; structures that are thought to have been created at the time of the separation of Africa and Antarctica.

The Anatolian Block and the evolution of the East and North Anatolian Faults

The collision of Arabia and Eurasia has caused much of the Anatolian Plateau to extrude to the west. The extruding block is bounded to the north by the right-lateral North Anatolian Fault and to the southeast by the left-lateral East Anatolian Fault (Fig. 3a). The East Anatolian Fault is 600 km long and extends from the Dead Sea Fault to the North Anatolian Fault (McKenzie 1972). Despite some small-scale complexity, it forms a nearly straight fault trace trending NE–SW (Fig. 3a; McKenzie 1976; Saroglu *et al.* 1988; Muehlberger & Gordon 1987). Lyberis *et al.* (1992) suggest that the East Anatolian Fault is an oblique collision belt, but this view does not appear to be correct. The East Anatolian Fault has accommodated mostly left-lateral slip (Saroglu *et al.* 1988; Westaway & Aeger 1996; McClusky *et al.* 2000; Khale *et al.* 2000) and crosscuts, west of Adana, folded structures related to the beginning of the Arabia-Eurasia collision (Westaway & Aeger 1996).

The North Anatolian Fault is a 1600 km long right-lateral fault with about 85 km total offset (Sengor *et al.* 1985; Westaway 1994; Hubert-Ferrari 1998; Barka *et al.* 2000). It extends from eastern Turkey to the Sea of Marmara as a single narrow zone along which a sequence of earthquakes of magnitude greater than 7 (Ketin 1969; Ambraseys 1970; Barka 1996) have occurred since 1939. The western part divides into two strands, the northern one being the most active (Barka & Kadinsky-Cade 1988; Armijo *et al.* 1999). The faults then enter the Aegean system, which has experienced modest extension (backarc stretching) for more than 15 Ma (e.g. Angelier *et al.* 1982; Mercier *et al.* 1989; Seyitoglu *et al.* 1992). Armijo *et al.* (1996) consider that the western extremity of the fault has enhanced the activity of NW–SE extensional basins to its west while suppressing activity to the east. The system can then be regarded as a vast damage zone associated with the propagating end of the North Anatolian Fault with the Gulf of Corinth being the basin most recently affected by the propagation process (Armijo *et al.* 1996, and see the later discussion).

Some information is available about the creation and earlier propagation of the North Anatolian Fault System. The shortening between Arabia and Eurasia started more than 30 Ma and resulted first in the closure of an ancient ocean, the Neotethys (Aktas & Robertson 1984; Michard *et al.* 1984; Hempton 1985). In a later phase collision occurred, resulting in uplift of the Anatolian Plateau about 12–15 Ma. This created major palaeogeographic, sedimentological and tectonic changes (Erinc 1953; Sengör & Kidd 1979; Dewey *et al.* 1986) with extensive volcanic activity (Yilmaz *et al.* 1987; Pearce *et al.* 1990) over the whole of eastern Turkey. The eastern part of the North Anatolian Fault seems to have formed soon afterwards (Sengor *et al.* 1985). Geological observations indicate that in its central part, movement on the North Anatolian Fault postdates 8.5 Ma (Hubert-Ferrari *et al.* 2002) and that, in its western part, around the Sea of Marmara, movement started about 5 Ma (Schindler 1998; Armijo *et al.* 1999) while further to the west, the Gulf of Corinth was reactivated at 1 Ma (Armijo *et al.* 1996). The propagation of the North Anatolian Fault from east to west at a rate of about 20 cm yr^{-1} is summarized in Fig. 4.

Contemporary deformation determined using GPS (Fig. 3a; Reilinger *et al.* 1997; Khale *et al.* 1999; McClusky *et al.* 2000) can, within the errors, be described by the rotation of the Anatolian plate around an Eulerian pole in the Sinai. Although providing no information about the evolution of the fault systems, this confirms that contemporary deformation is localised on the major faults. InSAR has also shown that strain accumulation across the eastern North Anatolian Fault is localised and consistent with slip at depth along a single fault (Wright *et al.* 2001).

In the Aegean, motion is not explained by Anatolian block movement (McClusky *et al.* 2000; Khale *et al.* 1999). Extension also occurs in Western Anatolia (e.g. Eyidogan 1988) and in the Aegean Sea (e.g. Jolivet *et al.* 1994; Avigad *et al.* 1998). Some authors thus consider the Aegean to be a separate microplate (e.g. Papazachos 1999) and infer that its motion is not solely related to the Arabian–Eurasian convergence and extrusion of the Anatolia (e.g. Kasapoglu & Toksoz 1983; Cianetti *et al.* 1997; Lundgren *et al.* 1998). Additional driving mechanisms such as slab-pull (Meijer & Wortel 1996, 1997) are also invoked.

Plasticine has been used by engineers to model plastic/brittle failure processes and was adopted by Peltzer *et al.* (1982) for the India-Eurasia collision (see also Tapponnier *et al.* 1982; Peltzer & Tapponnier 1988). To apply their results to the Anatolian system, we adopt a mirror image (east becomes west) of their model (Figs 3b and c). A rigid indentor deforms the plasticine with a free boundary situated to the west. The free boundary represents the subduction systems of the Hellenic-Cyprus arc. In the plasticine experiment, the first boundary to form was the left-lateral strike-slip fault that then propagated from the western border of the indentor toward the northeast (equivalent to the East Anatolian Fault). Once this fault had formed, a right-lateral strike-slip fault then propagated toward the free boundary (equivalent to the North Anatolian Fault). Both faults then continued to accommodate extrusion of the block toward the free boundary. In the plasticine models, once the faults were established, motion on them did not proceed smoothly, but switched between them (Peltzer *et al.* 1982).

MODELLING PROPAGATION

The structures that we model have been created by propagation and it is this process that we seek to understand. The concepts underlying our modelling are summarized in Fig. 5 which shows the evolution of opening (mode I) and shear (mode II) cracks subject to standard conditions for determining fracture toughness (Knott 1973; Lawn & Wilshaw 1975). Fig. 5(a) shows the extension of a pre-existing crack in a homogeneous medium such as glass or metal. When subjected to an opening stress, a mode I crack extends when the stress concentration at the tip (stress intensity factor) exceeds the fracture toughness (Knott 1973; Lawn & Wilshaw 1975). A pre-existing crack loaded in mode II however, sheds a mode I wing crack (e.g. King & Sammis 1991) preventing shear cracks from propagating.

Fig. 5(b) shows the same geometry for a material that contains small inhomogeneities either in the form of 'defects' or 'locked-in' stress inhomogeneities (e.g. King & Sammis 1991). The mode I crack propagates as before, but a substantial damage zone is created ahead of the advancing crack tip. For a sufficient density of defects or stress inhomogeneities, shear cracks can also propagate (Rudnicki 1980; Rundle & Klein 1989; Cowie & Scholz 1992a,b; Scholz *et al.* 1993) since substantial damage in the zone ahead of the tip results in a reduction of the effective elastic modulus. This allows shear

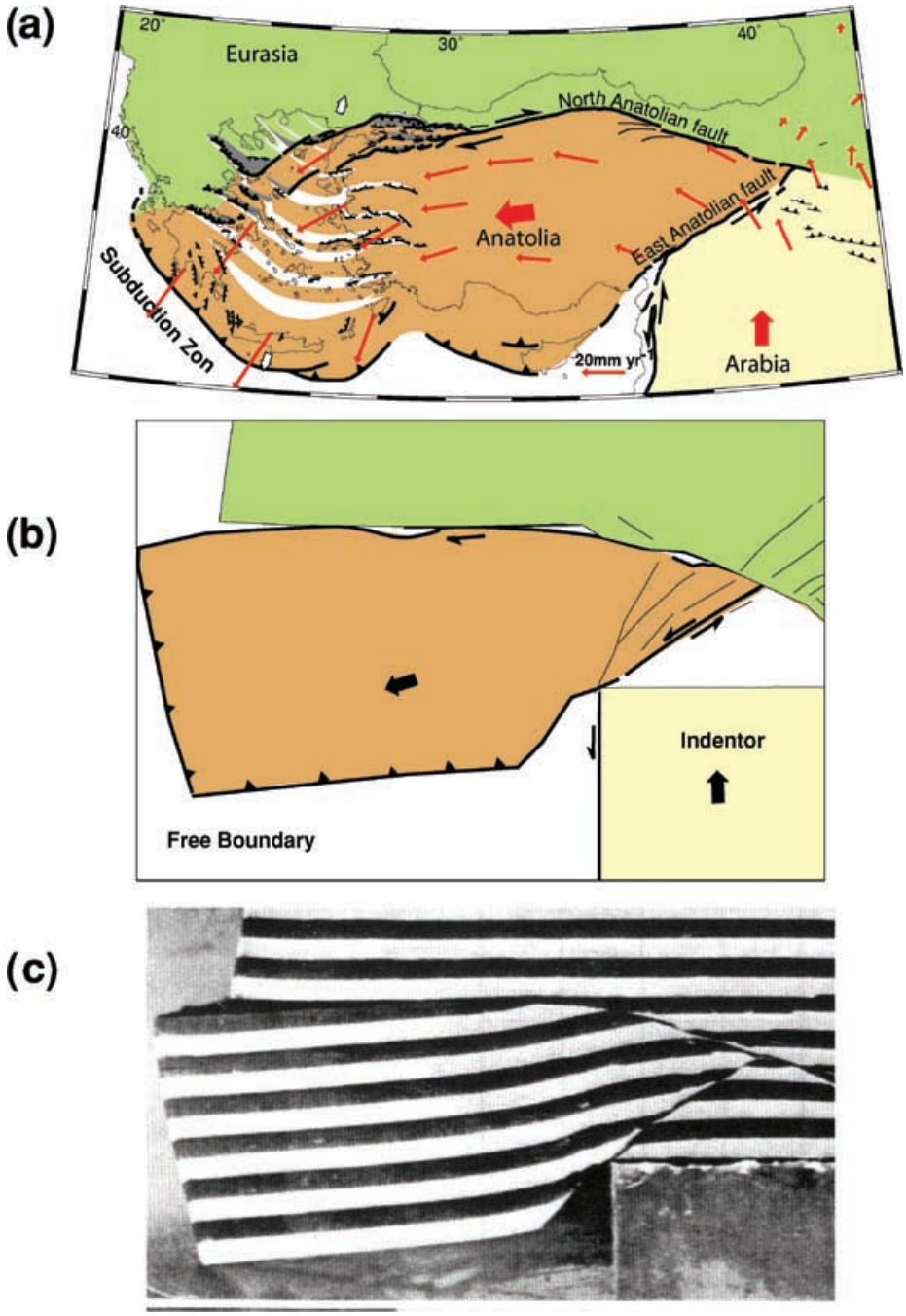

Figure 3. (a) Extrusion of Anatolia toward the Aegean subduction zone by movement along the North Anatolian and East Anatolian faults. GPS displacement vectors are shown (displacements relative to fixed Eurasia, Reilinger *et al.* 1997). Note east-west normal faulting in the Aegean related to backarc stretching and north-south normal faulting near the trench. (b) The Anatolian extrusion is similar to experiments in plasticine carried out by Peltzer *et al.* (1982). The indentor is applied to a free boundary at the base and the system is free to move westward. As deformation evolves a left-lateral fault first appears in the east. It is then cross cut by a right lateral fault that propagates toward the free boundary in the west. (c) A photograph of the original experiment.

to localise sufficiently for the mode II crack to propagate through the damage zone. Provided that the scale of the inhomogeneities is small, the resulting cracks propagate in a straight line and the system is predictable (Cowie & Scholz 1992a,b; Scholz *et al.* 1993; Meriaux *et al.* 1999; Lyakhovsky 2001). Concrete behaves in this way while pure cement behaves more like glass. Simple propagation concepts have been applied successfully to the propagation of ocean ridges where large-scale defects are generally absent in the ocean lithosphere (Morgan & Parmentier 1985; MacDonald *et al.* 1991).

The continental lithosphere is not homogeneous and large defects are present (from earlier episodes of deformation) as shown in Fig. 5(c). Propagation can only be understood if the defects can be defined and prediction of the failure process is impossible from simple boundary conditions alone. For this reason, such materials are avoided for engineering purposes and more sophisticated

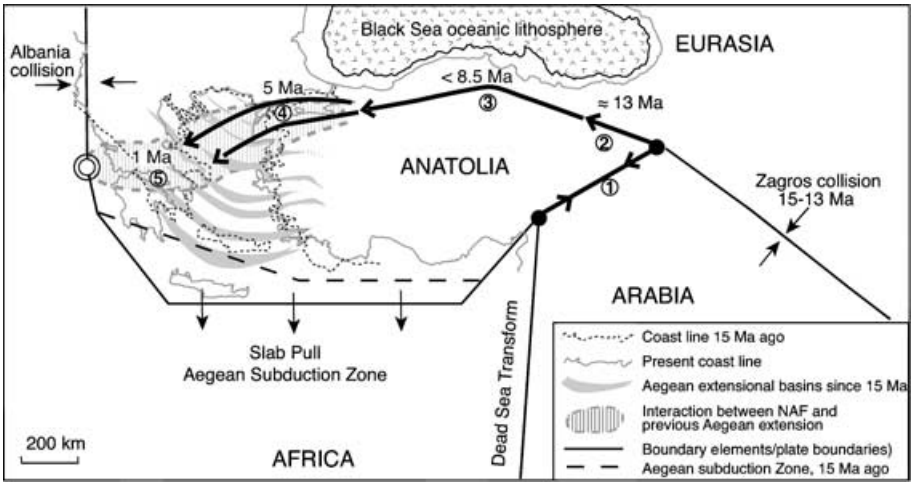

Figure 4. Propagation of the North Anatolian Fault (NAF). Initiated in the east during the uplift of the Anatolian Plateau and after the formation of the East Anatolian Fault (1, 2). The NAF propagated across north Anatolia (3) and reached the Marmara Sea 5 Ma ago (4) and the Gulf of Corinth 1 Ma ago (5). When the NAF entered the Aegean region, it interacted with the existing active extensional structures. The shape of the NAF is parallel to the Black Sea oceanic lithosphere. Black lines represent present plate-boundary geometry as introduced in the modelling. The present (gray) and past (dashed, Armijo *et al.* 1996), coastlines of Greece and Western Turkey are indicated.

modelling techniques developed by engineers are not well adapted to studying Earth problems in a predictive way. Nonetheless, simple modelling can be applied retrospectively to understand how structures have evolved. Features that have resulted from the loading or boundary conditions can be distinguished from those that must be the consequence of pre-existing defects. Furthermore it is possible to determine why a feature should have propagated in one direction rather than another. Elastic models over estimate stresses in the process zone around crack tips since the material loses strength (e.g. Cowie & Scholz 1992a,b; Lyakhovsky 2001) and for the same reason strain amplitudes are slightly underestimated. Nonetheless since principal axis directions are approximately correct, the future directions of new faults can be predicted well enough from an elastic model.

The models in Figures 5(a)–(c) require elastic behaviour and strain weakening. If the material is viscoelastic (Fig. 5d.) then propagation will only occur if the loading generates stress more rapidly than it can relax, otherwise deformation becomes distributed. The relaxation time of the material determines which behaviour predominates and viscous deformation and crack propagation co-exist only near to the transition. For example, it is very difficult to make 'silly putty' both crack and flow at the same time. While many Earth materials exhibit strain hardening for small strains (Agnon & Eidelman 1991), several processes can result in strain softening when deformation becomes substantial (e.g. Peltzer & Tapponnier 1988). These include the weakening effects of water or other fluids (e.g. Pili *et al.* 1997a,b), changes of crystal size with deformation, shearing along weak planes of less resistant crystals (e.g. Poirier 1980; Braun *et al.* 1999) and increases of temperature due to shear heating (e.g. Barr & Dahlen 1989; Molnar & England 1990; Nicolas *et al.* 1977; Scholz 1980). Strain softening can also suppress power law creep observed for the same material under laboratory conditions. This is illustrated in Fig. 6. Stresses sufficient to cause viscous flow become restricted to the damage zones so that the bulk of the material appears elasto-plastic particularly in the presence of pre-existing defects. McClintock (1971) discusses the formation of elastic-brittle (sic) structures in materials that laboratory tests suggest should exhibit distributed deformation.

It seems that at a large scale the Earth's lithosphere behaves in many respects as if it were an elastic-brittle material and the clearest evidence for the correctness of such a hypothesis is field evidence of large-scale propagation. Extrapolating from small-scale laboratory experiments that show power law creep is not a reliable method of determining the large-scale behaviour and should not be assumed to be the key evidence for lithosphere rheology. Evidence for rocks deformed by ductile flow can be found throughout the crust, but these can be formed in large process zones or shear zones. Elastic-brittle behaviour only requires that the dimensions of regions that, at any time, remain elastic greatly exceed those experiencing ductile deformation. Major faults have been repeatedly created and propagated through continental lithosphere so that most of it has been, at some time, in the process zone of a propagating structure.

Creating propagation models

We examine propagation over many hundreds of kilometres, distances much greater than the lithospheric thickness and therefore adopt an elastic plate model (e.g. Bilham & King 1989). This distinguishes our approach from similar more local studies (e.g. Gomberg 1993; Katzman *et al.* 1995; Ten Brink *et al.* 1996) for which 3-D effects are potentially important. These studies assume that the bulk of the medium can be regarded as elastic except where localised shear or opening occurs and that the permanent deformation associated with process or damage zones, even when they are relatively large, can be neglected. The overall justification for our elastic approach lies in the absence of significant long-term internal deformation of the plates. For the Gulf of Aden, the magnetic anomalies and rift flanks are undeformed since the rift was established (Manighetti *et al.* 1997). Necking occurred (Fantozzi 1996; Hébert *et al.* 2001) prior to ocean floor spreading and is consistent with the passage of a process zone discussed later. Similarly in Anatolia, no substantial geological (Hubert-Ferrari *et al.* 2002) or geodetic (McClusky *et al.* 2000) deformation occurs away from the main faults although evidence for more distributed deformation associated with propagation processes exists (Armijo *et al.* 1999; Hubert-Ferrari *et al.* 2002). The elastic modelling is carried out using a 2-D boundary

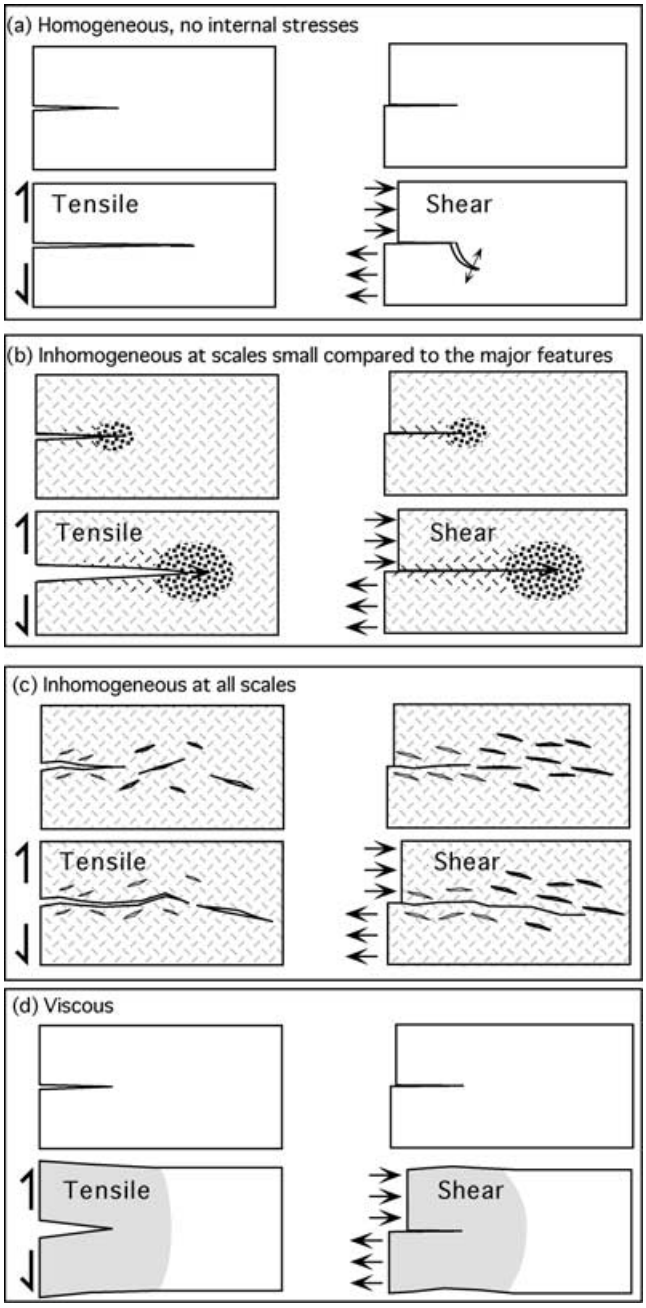

Figure 5. The propagation of tensile and shear fractures subject to simple boundary conditions. In each panel the figures on the left are for tensile (mode I) failure and those on the right for shear (mode II) failure. The upper pair of figures in each panel shows pre-fracturing before a load is applied. (a) Loading of a homogeneous material. The mode I crack can propagate but the mode II crack cannot. (b) Loading of an inhomogeneous material. The size of the largest inhomogeneities or defects is small compared to the size of the pre-fracture. Mode I fractures propagate. Mode II can also propagate under certain circumstances (see text). (c) Loading of a material that is inhomogeneous at all scales. The largest defects dominate the fracture process if they are orientated such that they are appropriately stressed by the advancing rupture front. The evolution of deformation in such a material requires knowledge of these defects or a large number of examples so that the behaviour can be studied statistically. Neither is possible for continental lithosphere and propagating features can only be studied retrospectively. (d) Loading of elasto-brittle or elasto-plastic material that also exhibits viscous behaviour. If the loading rate is slower than the viscous relaxation rate the crack will not propagate.

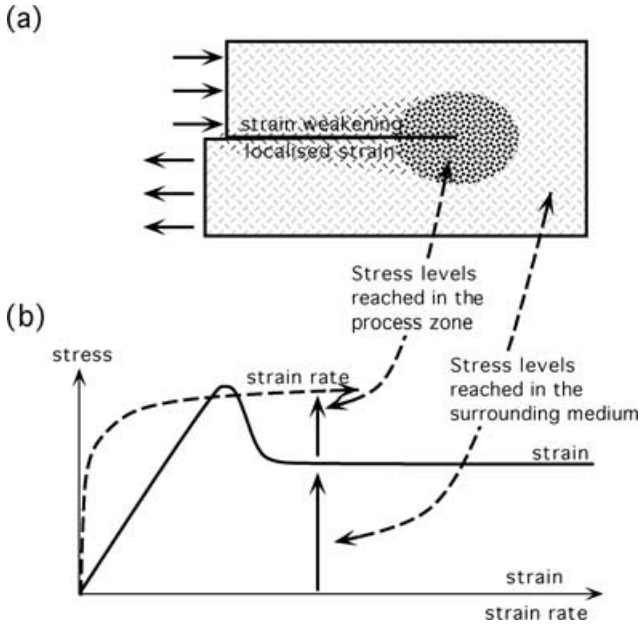

Figure 6. Stress vs strain and strain-rate curves for a plastic strain weakening material that also exhibits power law creep (non-linear viscous behaviour). The solid line indicates the elasto-plastic behaviour and the dashed line power law creep. In such a medium, once slip planes are created only material in the process (damage zone) of the advancing crack (or fault) tip can reach stress levels at which viscous flow becomes significant. The rest of the material is in the 'shadow' of the weak fault. For significant deformation such a material behaves as if it is elasto-plastic even though for limited deformation it may appear viscous (McClintock 1971). If the material contains pre-existing defects, even limited deformation will not cause viscous deformation except close to the crack tips.

element code (Crouch & Starfield 1983). This allows us to apply both realistic boundary conditions based on known plate geometries and plate motions, and also to examine complex fault geometries.

To determine where evolving failure will occur a failure criterion is required. For tensile failure this is straightforward; failure is promoted by normal stress. The choice of a shear failure criterion is less straightforward. When solids fail in shear they almost invariably expand. This is true even when the microscopic processes of creating dislocations in crystals is considered (Naborro 1967). The dilatancy effect is very modest in metals, but this dilatancy is more dramatic when rocks or ceramics are sheared. It follows that confining pressure, by suppressing dilatancy, tends to inhibit shear. Thus shear failure is a function of confining pressure as well as shear stress. When observed between two pre-existing surfaces the effect is described as friction. In this case the two surfaces can slip more readily if they are permitted to move apart slightly (Bowden & Tabor 1950, 1964). The concept of friction is also applied to the failure of materials that are not pre-fractured, but is re-named 'Internal Friction' or 'Coulomb Failure'. The friction or Coulomb failure criteria adopted is defined in Appendix 1.

The Gulf of Aden

Fig. 7(a) shows the Gulf of Aden region and model. The present geometry is not the same as when the Aden rift initiated and two changes must be made to reproduce the original geometry. First, Arabia is displaced to fit against the coasts of Somalia and Africa by motion in the opposite direction to opening (white arrows). The

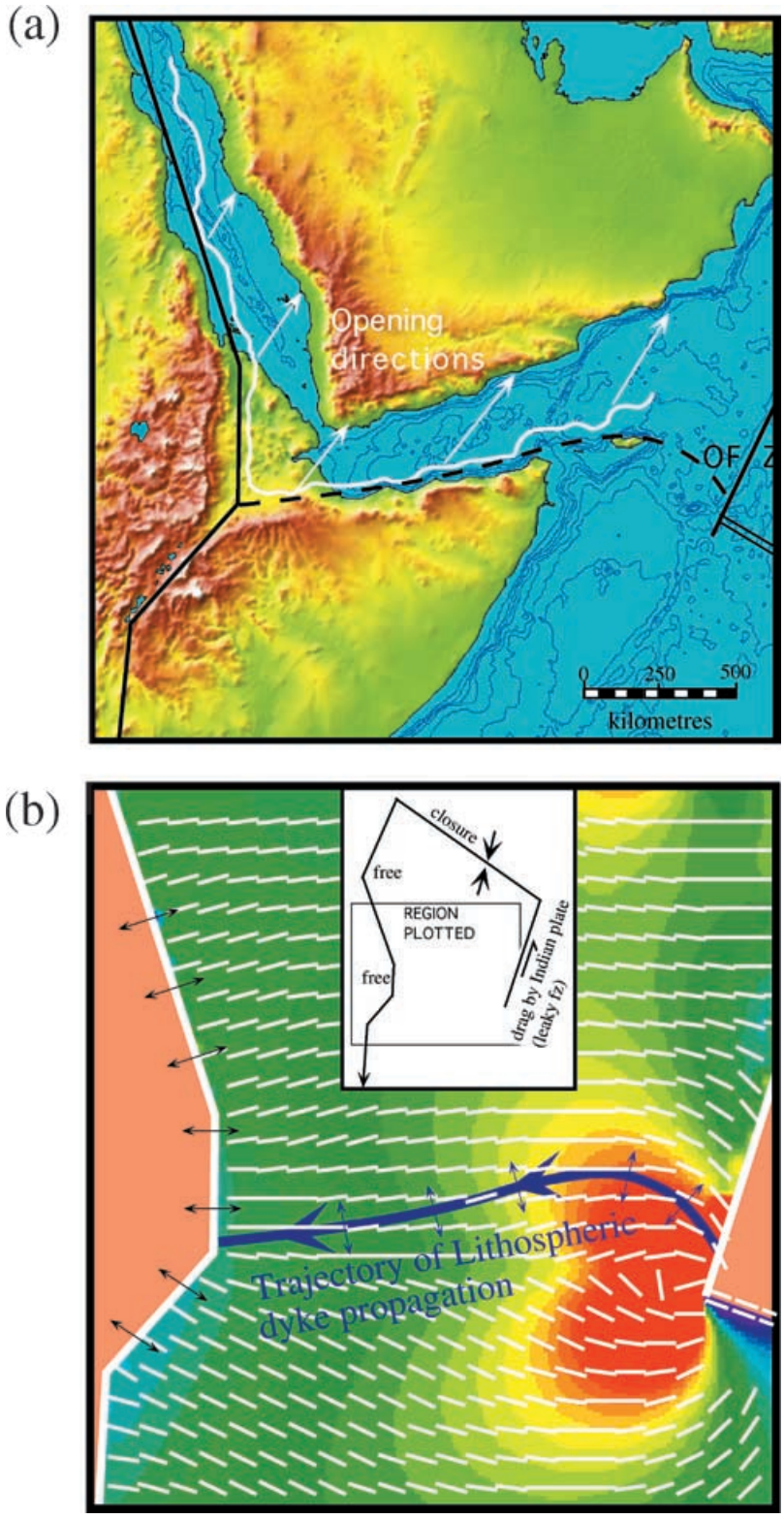

Figure 7. Modelling the opening of the Gulf of Aden. (a) A present day map of the region. In white, the original position of the Arabian coast rotated back around the pole of rotation. A dashed black line shows the locus of initial fracture for the Gulf of Aden. OFZ: Owen Fracture Zone. (b) Inset shows the applied boundary conditions (Appendix 2) for the initial geometry described in (a). The model shows increased extensional stress as red shades and reduced stress as mauve or blue. The amplitudes are arbitrary. White lines indicate the directions favoured for the formation of dykes or normal faults. The model is mostly sensitive to boundary orientation. The strike-slip Owen Fracture zone requires one principal axis to lie at 45° to the fracture axis. This defines the form of the eastern Gulf of Aden. Close to the East African rift and Proto-Red Sea boundaries, one principal axis must be perpendicular to these structures. Principal axes therefore converge towards the Afar requiring that the ridge propagate toward this region. The locus of initial fracture (thick blue line, taken from (a) and the initial direction of propagation (arrow) are superimposed.

narrow zone between the restored coasts defines the path of the Aden Rift when it first propagated. The second change is to restore the original position of the Carlsberg ridge axis by shifting it NNE by half the total spreading. The length of the Owen Fracture zone is correspondingly decreased.

The boundaries used in the model are shown in the inset to Fig. 7(b) and the parameters used are described in Appendix 2. The East African Rift and Proto-Red Sea are treated as free boundaries, thus assuming that the boundaries are 'weak' (Bercovici 1996; Tackley 1998) and transmit no significant shear stress. This fixes one principal stress axis to be perpendicular to these boundaries. The northern boundary, corresponding to the Zagros, has slip imposed in the appropriate plate direction with an increase from west to east, to account for changing distance from the rotation pole. Slip along the southern Owen Fracture zone is constrained to be strike-slip in the south and left free in the north. The Dead Sea Fault is similarly constrained.

The Anatolian System

To model the collision of Arabia and Eurasia, displacement is imposed on the boundary elements representing the Arabian side of the Zagros. The Aegean subduction is modelled by boundary elements that allow it to displace freely. Setting this plate boundary as a free boundary is necessary to allow material to move toward the Aegean trench. We do not explicitly introduce slab-pull in the first models because its importance is an open question and because alone it cannot account for the east to west propagation of the North Anatolian Fault although it can account for the stretching (backarc) in the Aegean between 15 and 5 Ma and some of the present deformation. Unlike the plasticine model (Figs 3b and c) where the western boundary is completely stress free, the region north of the Hellenic subduction zone (NW Greece and Albania) is prevented from moving by fixed elements to simulate the collision which occurs in this area. The location of all the boundary elements is described in Appendix 2 and the inset in Fig. 10(a). Using the present-day geometry of the Africa–Anatolia and Anatolia–Eurasia plate-boundaries is not strictly correct. Fig. 4 shows the approximate location of the Africa and Anatolia boundary at 15 Ma. However, the $\sim$100 km cumulative displacement of the Anatolian faults has not changed their geometries significantly. Thus, unlike the Gulf of Aden where the reconstructed geometry was required, the present day geometry can serve for modelling.

THE RESULTS OF THE MODELLING

Aden ridge propagation

The modelled extensional stresses are shown in Fig. 7(b) with red colours indicating increased tensile stress and short white lines indicating the optimum orientation for Mode I failure (dyke, normal fault or rift formation). The model exhibits three main features. First, the white lines are everywhere perpendicular to the stress free boundaries. Consequently they converge towards the two bends in the African rift–Red Sea rift system in the Afar region. Second, the white lines approach the strike-slip boundary of the Owen Fracture zone at 45°. Third, the greatest Coulomb stresses are associated with the Carlsberg ridge–Owen Fracture zone junction. These features are all a simple consequence of the applied boundary conditions (see caption to Fig. 7b). It is important to note that the predicted fracture directions are not, in general, perpendicular to the direction in which the Arabian plate will move once fracture has occurred.

Superimposed on the model (Fig. 7b) is a smoothed form of the initial rift trajectory (from Fig. 7a). It started in a region of high extensional stress and then followed a trajectory that led to the point where it is observed to arrive at the African rift–Red Sea rift junction (present day Afar). The form is thus consistent with the elastic model. Although other initiation points could have been possible, any trajectory initiating to the north of the Carlsberg ridge would start with a smoothly curved section like the Sheba ridge. Furthermore, all initiation points would arrive near to the African rift—Red Sea rift junction since fracture directions converge towards the bend in the rift system. Extensional stresses promoting fracture are greater at the eastern end of the incipient fracture and thus, the model is consistent with the observed east to west propagation of the Aden rift. We show only the initial stage in the propagation process in the figure since detailed modelling by progressive addition of opening elements does not change the propagation path. As discussed later for Anatolia, this is not generally the case for propagating systems.

A mechanism (modified from Abelson & Agnon 1997, 2001) that explains why the rift should change from being essentially unsegmented, when passing through oceanic crust to being segmented when it encounters continental crust is summarized in Fig. 8. When the initial tensional crack (or dyke) cuts the mantle it follows a track perpendicular to the maximum extensional stress (the curved trajectory of Fig. 7b). In oceanic regions magma buoyancy is sufficient for the ridge (2 km below sea level) to be created at the same time as the mantle dyke and thus has the same form, but in continental lithosphere, magma buoyancy is inadequate to lift magma to the surface ($>$1 km above sea level) and a volcanic ridge does not form immediately (Fig. 8a). As a consequence, normal faults and grabens must accommodate deformation until the crust is sufficiently thinned for magma to approach the surface. This process creates what may be regarded as a large damage zone associated with upward propagation, delaying the appearance of a simple oceanic ridge.

Only after the mantle dyke is formed are the crustal structures created. Once formed, the mantle dyke opens obliquely, in the direction of motion of Arabian relative to Somalia and thus the upward propagation and fault formation occurs in a stress field rotated with respect to the one that created the mantle dyke (Fig. 8b). The normal faults and grabens created strike at right angles to the opening vector of the mantle dyke and hence form en echeon segments (Abelson & Agnon 1997). In the west, as the 'hotspot' is approached, magma pressures are higher partly suppressing faulting and the ridge becomes arcuate as in the east.

While these mechanisms can explain small en echelon features, they cannot explain much larger ones such as the Socotra or Alula Fartak transforms. These features appear to be related to reactivation of pre-existing structures. To examine reactivation, we calculate the stress associated with such an interaction. Stresses are calculated for optimally oriented faults using the boundary conditions in Fig. 7(b). The Coulomb failure criterion is used on the understanding that dykes are promoted under similar conditions to normal faults (see caption to Fig. 9). When the ridge arrives at a pre-existing structure, the part south of the intersection can be activated as a right-lateral strike-slip feature (Fig. 9a). The stress tending to activate strike-slip faulting is comparable to that for continued propagation of the ridge. Therefore to be reactivated, the pre-existing feature does not have to be very weak. When fault slip occurs (Fig. 9b), shear stress is concentrated at the end of the reactivated fault such that it extends further. Stresses of similar magnitude, but favouring normal

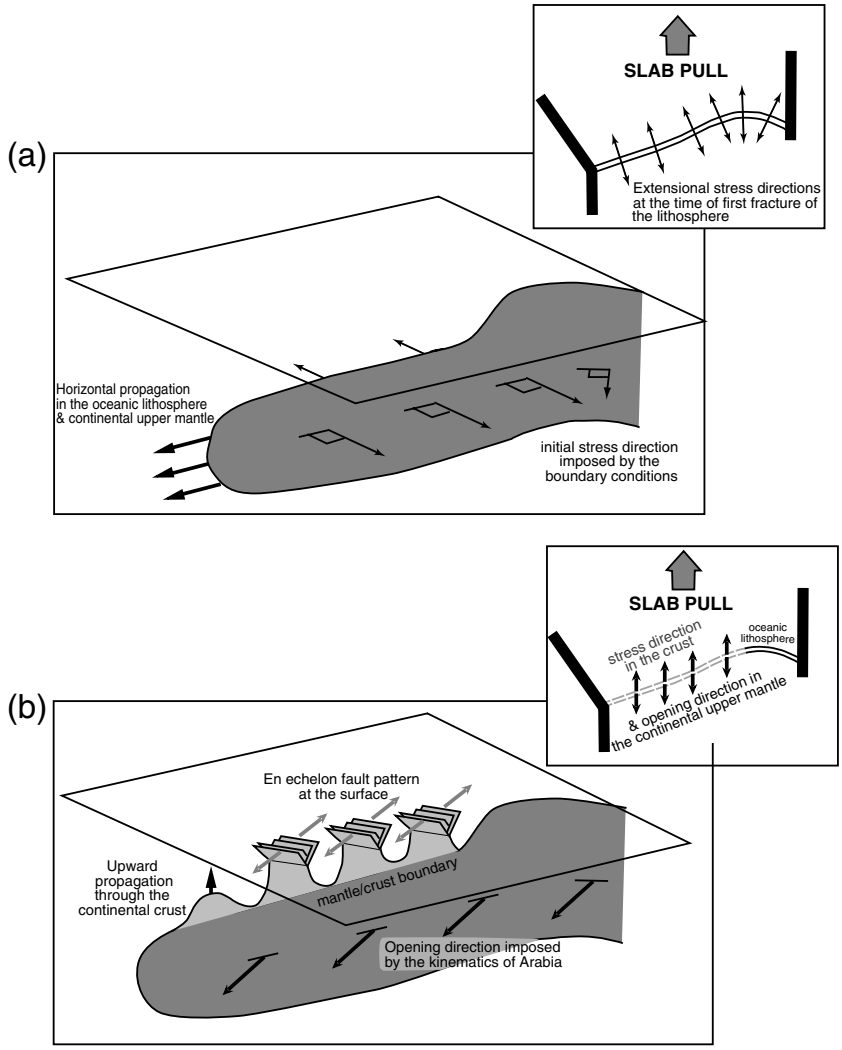

Figure 8. The formation of small en echelon features. (a) The initial failure in the upper mantle following the stress trajectory shown in Fig. 7. Failure extends to the surface for oceanic lithosphere, but fails to reach the surface in continental lithosphere. (b) Once fracture has occurred, the opening direction is kinematically determined by the direction of motion of the new Arabian Plate. This opening is oblique to the initial fracture and generates extensional stress directions in the crust that are rotated relative to the stresses that created the upper-mantle fracture. Upward propagation of rupture in the continental crust occurring in this oblique stress field creates en echelon fault/ridge segments.

or oblique faulting develop along its western side. The process of distributing stress over a broad region allows the eastern part of the ridge to continue to open without further westward propagation. As the transform fault becomes longer however, the stresses tending to extend it diminish relative to the stresses promoting normal faulting or dyking and eventually a new ridge is created on the western side. Since stresses are distributed, the modelling does not define where new westward propagation will initiate; it will start from an appropriate defect. While not defining exactly how large the offsets should be, the process explains how large offsets can be created and why the propagation of the Aden ridge could have been delayed by several million years where they occur.

East and North Anatolian Fault propagation

Fig. 10 shows the evolution of the Anatolian system. For the beginning of the collision only the boundary elements in black are introduced (inset Fig. 10a) and the resulting Coulomb stress produced by shortening in the Zagros area is calculated (Fig. 10a). Then boundary elements (in white) representing the East Anatolian Fault (Fig. 10b), the eastern (Fig. 10c) and central parts (Fig. 10d) of the North Anatolian Fault are progressively added to the model.

Initially, the Coulomb stress increase is concentrated between the Dead Sea fault and the Zagros (Fig. 10a). In this area, optimum left-lateral faults have a fairly constant NE–SW orientation and the stress model tightly constrains the potential trajectory of the East Anatolian Fault. The East Anatolian Fault is located in an area of stress increase and its strike is similar to the optimum fault orientations. The highest stresses are at the ends of the future fault that might therefore be expected to develop by propagation from both ends (shown by arrows in Fig. 10a).

After the collision, the East Anatolian Fault is added as a free slipping fault (Fig. 10b). As a result, the Coulomb stresses increase at the eastern end of this element. In this area, the optimum right-lateral faults have a NW–SE orientation. Further west, optimum fault orientations rotate to become first E–W and then NE–SW. The

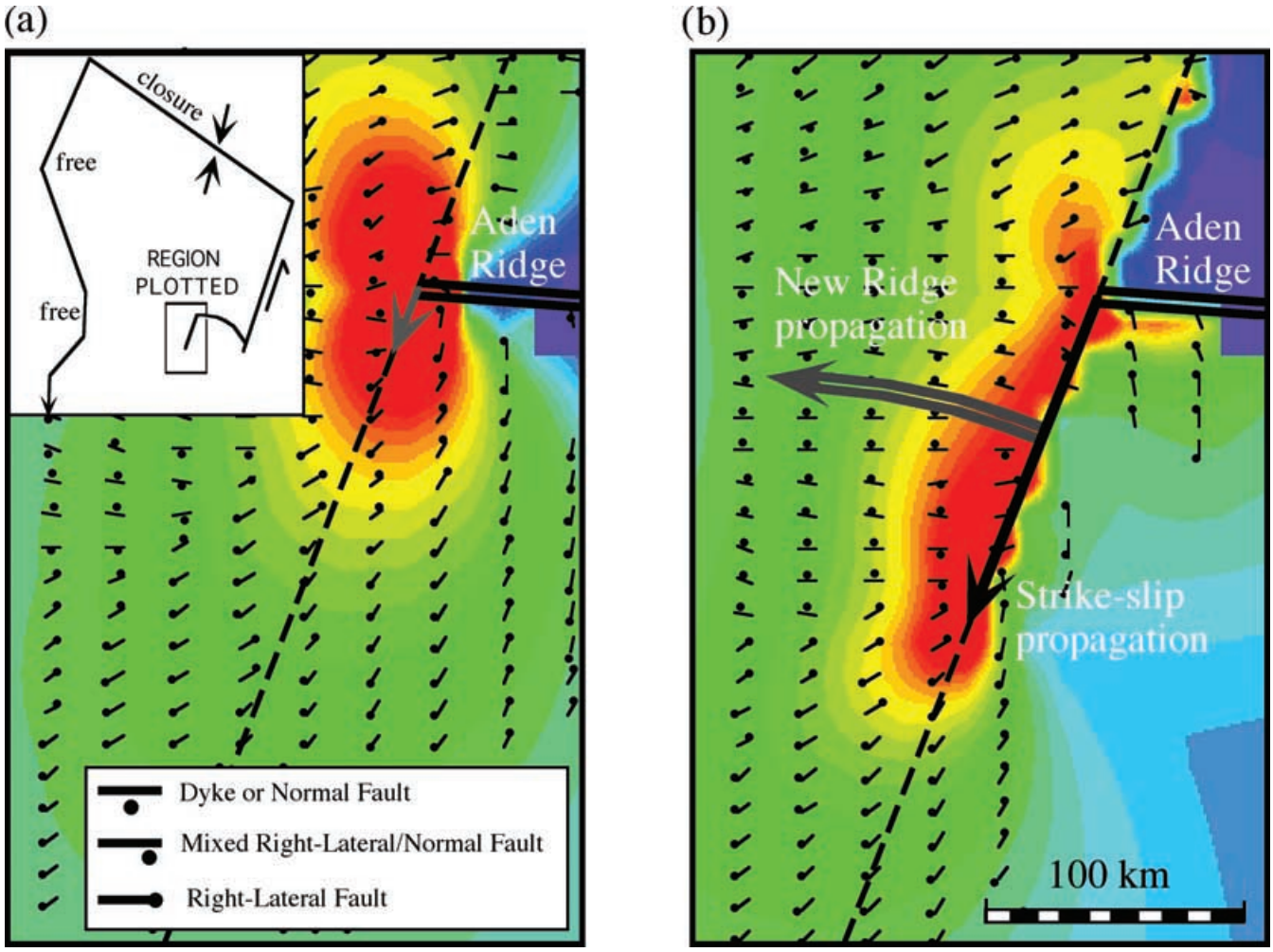

Figure 9. The effect of a propagating ridge encountering a pre-existing structure (dashed line). The Coulomb stresses are for faults with optimally orientated strike, dip and rake. This differs from the earlier calculation, which calculated optimum directions for normal faults or dykes alone. Normal faults and dykes are created under the same conditions except for fluid pressure. If magma pressure is sufficiently high dykes and not normal faults will be formed. Attempting to quantify this effect is beyond the scope of this paper, but the qualitative processes described should remain the same. The type of faulting is identified in the bottom inset in (a). Upper inset shows the applied boundary conditions. (a) The Coulomb stresses promoting continued eastward normal fault or dyke propagation are similar to those promoting strike-slip faulting along the pre-existing structure. Such a feature can thus be re-activated as a strike-slip fault. Motion on the strike-slip fault allows continued opening on the Aden ridge to the east. (b) As the strike-slip fault extends, the zone of high stresses at the fault tip causing it to extend are diminished relative to high stresses encouraging normal faulting or dyking which develop along the western side of the fault. Finally a new ridge begins to propagate.

present-day geometry of the North Anatolian Fault is consistent with these orientations. As the greatest increase in Coulomb stress is in the east, fracturing may be expected to have started there. Thus, whatever other effects may modify propagation further to the west, this alone is sufficient to explain why propagation started in the east. Eastern Anatolia is distant from the Hellenic arc and slab-pull along the arc produces insignificant shear stresses in the region. Thus it cannot explain east to west evolution of the fault system.

As discussed for the Gulf of Aden, the solution is not unique, although all other initial trajectories would tend to converge towards the subduction zone. Any trajectory starting to the north-west of the Zagros would have an initial north-west direction. Furthermore, most initial trajectories would converge toward the junction between the subduction zone and the locked zone in Albania. The bend of the North Anatolian Fault in its central part is more pronounced than the optimum fault directions suggest and seems to follow the Black Sea coastline. As we have seen for the Gulf of Aden, lithospheric inhomogeneities influence both the geometry of the propagating ridge and the timing of the propagation. In northern Turkey, it seems possible that pre-existing features have had some influence on the path of the North Anatolian Fault (see later discussion).

In Fig. 10(c), the eastern part of the North Anatolian Fault is introduced with the result that Coulomb stresses increase at the western extremity of the element. The orientation of optimum right-lateral faults hardly changes and the North Anatolian Fault can continue propagating to the west. Figs 10(b) and (c) also indicate that Coulomb stresses increase north of the North Anatolian Fault in its eastern part. In this area the optimum left-lateral faults have a NE–SW orientation that corresponds to observed left-lateral faults (Saroglu & Guner 1981; Barka *et al.* 1983, 1985). In Fig. 10(d), a

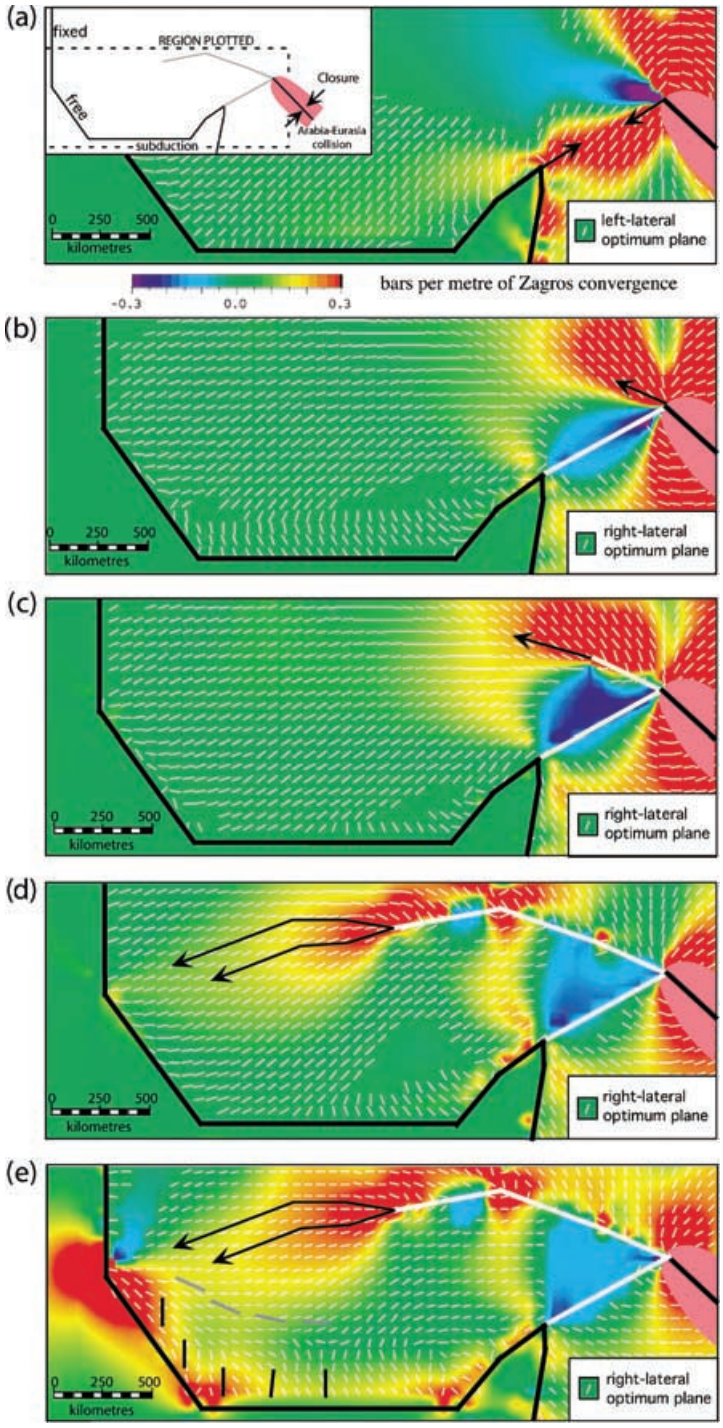

Figure 10. Coulomb stresses associated with the creation and propagation of the Anatolian faults. The stresses are for Coulomb shear failure with red shading indicating stress increase. The inset shows the geometry of the boundary elements (more detail in Appendix 2). The North and East Anatolian faults are sequentially added in the model. (a) Boundary elements introduced in the modelling correspond to the black lines in the inset. The resulting increase in Coulomb stress and the associated left-lateral optimum faults (short white lines) are compatible with the creation of the East Anatolian Fault. The highest Coulomb Stresses occur at either end of the future East Anatolian Fault. This suggests that fault propagation occurred simultaneously from both ends. There is no geological information to confirm this. (b) The East Anatolian Fault is added as a freely-slipping element. As a result, the stresses and the optimum right-lateral fault orientations (short white lines) change. They are now compatible with a westward propagation of the North Anatolian Fault. (c) The eastern part of the North Anatolian Fault is added as a freely-slipping element. As a result, stress increases at its western extremity, enhancing westward fault propagation. As in (b), the Coulomb stress increase NE of the fault is compatible with the propagation of left-lateral faults similar to those observed. (d) The eastern and central parts of the North Anatolian Fault are introduced as freely-slipping elements. The observed propagation of the North and South branches of the North Anatolian Fault into the Aegean is compatible with the produced stresses. (e) To account for probable slab pull induced by the Aegean subduction zone, a small contraction is imposed along the subduction zone (10 per cent of that imposed in the Caucusus-Zagros). Slab-pull enhances the tendency seen in (d) for the North Anatolian Fault to propagate into the Aegean. It also changes the stress field near the trench such that E–W normal faulting (grey lines) is expected in the Aegean and N–S normal faulting (black lines) near the trench. These optimum normal fault strikes are compatible with the present deformation (Fig. 3).

free boundary element representing the extension of the North Anatolian Fault to the Sea of Marmara is introduced. Coulomb stress is now increased between the North Anatolian Fault and the junction between the subduction zone and the Albanian locked zone (Fig. 10d).

In the preceding models, we have modelled the subduction zone as a free boundary. However, slab-pull is often considered as an important effect in the Anatolian extrusion process (e.g. Kasapoglu & Toksoz 1983). While it is too distant to modify the early stages of the evolution of the North Anatolian Fault, it certainly influences mechanical processes in the Aegean. In the final model we impose a small north-south shortening across the elements representing Aegean subduction. The resulting Coulomb stresses are increased (compare Fig. 10e to Fig. 10d). The optimum right-lateral fault direction does not change in the North Anatolian Fault area, but stresses south of the North Anatolian Fault are more compatible with present day activity. North-south normal faulting is predicted by the model close to the trench. Further north, east-west normal faulting is predicted. A similar distribution of major active normal faults of the southern Aegean is observed (Fig. 3; Lyon-Caen H. *et al.* 1988; Armijo *et al.* 1992). Thus slab pull seems to enhance the westward propagation of the North Anatolian Fault across the Aegean Sea and explain the form of normal faulting perpendicular to the Hellenic Arc.

The modelling gives further clues to the mechanisms of extrusion. At first, the stress field induced by the northward movement of Arabia (contraction in the Zagros range and left-lateral movement along the Dead Sea fault) increases stress in the area of the East Anatolian Fault. Only when the stress is released by allowing the fault to move do stresses increase along the future trend of the North Anatolian Fault. The evolution thus proceeds in steps. First the East Anatolian Fault is formed, followed by the creation of the North Anatolian Fault. More generally, with continued evolution of the two faults, simultaneous motion is not to be expected. Exactly how such temporal interactions operate depends on details of the changes of the fault geometry (notably at bends or junctions) as finite strain accumulates and on healing processes. These topics are beyond the scope of this paper and are under investigation using a combination of plasticine and numerical modelling.

Short term evidence for such activity transfer between the East and North Anatolian faults may be found in the historical seismicity (Ambraseys 1970; Ambraseys 1971; Ambraseys 1989; Ambraseys & Melville 1982; Ambraseys & Melville 1995). Fig. 11(a) shows that from 100 AD to 500 AD the East Anatolian Fault was relatively inactive and the North Anatolian Fault was active. Activity then switched, with the East Anatolian Fault becoming the most active. In 1150 activity returned to the North Anatolian Fault. Similar features are also observed in the more recent history (Fig. 11b). In 1668 a sequence of events propagated from east to west along the North Anatolian Fault reaching the Western Sea of Marmara in 1766. The East Anatolian Fault was then active with a series of large events between 1789 and 1893. The North Anatolian Fault again became active in 1939 with a sequence that again propagated from east to west, and continues to the present-day Hubert-Ferrari *et al.* (2000). The East Anatolian Fault sequence started at each end of the fault and propagated towards its centre (Fig. 11b). The North Anatolian Fault sequences have all propagated from east to west. This behaviour is consistent with the fault switching inferred from Coulomb modelling. The Stress modelling might be interpreted to suggest that the entire East Anatolian Fault was created before North Anatolian Fault came into existence. It seems more reasonable to suppose that activity has repeatedly switched back and forth to progressively create the faults.

DISCUSSION

Pre-existing inhomogeneities

In both the Gulf of Aden and Anatolia, pre-existing inhomogeneities influence the direction of propagation. Once initiated, the path of the Aden ridge is determined, but a pre-existing feature of the ocean lithosphere must have controlled the initiation. As it propagated, structures parallel to the African coast appear to have delayed propagation and created the larger ridge offsets. The path of North Anatolian Fault also responded to pre-existing conditions. For much of its length it runs parallel to the Black Sea coast. While this is close to the optimum failure direction, it is not exactly so, suggesting that the propagating fault may have been influenced by other structures.

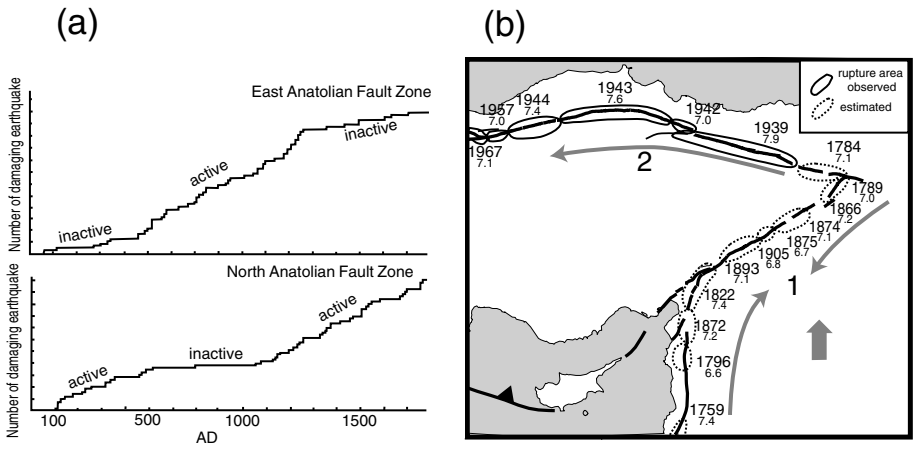

Figure 11. (a) The time distribution of damaging earthquakes. When the East Anatolian Fault (top) is inactive, the North Anatolian Fault (bottom) is active and vice versa (modified from Ambraseys 1971). (b) Earthquakes of magnitude greater than 7.0 along the northern part of the Dead Sea fault and the East and North Anatolian faults. Activity along the East Anatolian Fault is followed by activity along the North Anatolian Fault. A North Anatolian Fault sequence immediately preceding that on the East Anatolian Fault is discussed in the text. North Anatolian Fault sequences apparently propagate from east to west while that on the East Anatolian Fault sequence propagates from the fault ends towards the centre. This is consistent with Coulomb models (Figs 10a and b).

There are three possibilities. First, the rigid Black Sea oceanic lithosphere may resist penetration by a propagating fault, either because it modifies stress trajectories or because it is too tough to fracture. Second, the coast is controlled by structures formed during the Cretaceous to early Eocene compressional phase and associated inland structures may have tended to deflect the fault slightly. Third, the topographic gradient between the land and sea modifies the lithospheric normal stress parallel to the coast. Molnar & Lyon-Caen (1988) discuss this effect in relation to mountain building. Lower normal stress predicted by their model would occur inland from the Black Sea coast at the present location of the North Anatolian Fault. It is not straightforward to distinguish between these possibilities. However, the Dead Sea fault and the San Andreas for much of their lengths follow paths a similar distance inland from their associated coastlines suggesting that low normal stress may be the explanation.

Evolution of the Aegean

The inhomogeneities described above are essentially passive stress fields or material property differences inherited from earlier and now extinct phases of deformation. We now consider the more complex case of the North Anatolian Fault entering the Aegean region. As discussed earlier, Aegean extension was active when the North Anatolian Fault reached the Marmara region about 5 Ma. The North Anatolian Fault then encountered a series of major pre-existing structures and a different stress environment to that in east and central Anatolia. Fig. 12(a) (modified from Armijo *et al.* 1996) shows the Aegean area with orange bands indicating the form of the extensional features that existed prior to the arrival of the North Anatolian Fault.

The altered stress regime caused the extending fault to be deflected to the north. It is this change in direction relative to the fault slip vector that has caused the Marmara Sea to open as a pull-apart (Armijo *et al.* 1999, 2002). Further to the southwest, the propagating fault has reactivated (or increased the activity of) a series of pre-existing grabens of which the Gulfs of Evvia and Corinth are the most recent. Unlike the Sea of Marmara where all of the extension is associated with the pull-apart process, the proto Gulfs of Evvia and Corinth were substantial features before reactivation. The underlying mechanical processes can be appreciated from the two insets (Fig. 12b). The upper right shows a shear crack propagating into a region where the extension direction is nearly normal to the propagation direction. New cracks are created subparallel to the propagating fault. This is comparable to the situation encountered when the North Anatolian Fault reached the Sea of Marmara region. The upper left inset shows a shear fault entering a region where the extension axis is at more than 45° to the propagation direction. This reactivates pre-existing fissures orientated at a high angle to the fault and is comparable to the reactivation of the grabens of the western Aegean.

The insets show centimetre-scale field examples, but they emphasize a feature common to all propagating systems. A propagating shear fault can enter a region where the stress regime is different from that which drives it and can reactivate or initiate structures that are appropriate to that stress system. The small-scale examples can only be understood in this way. Similarly, the North Anatolian Fault is driven by collision processes in eastern Anatolia not by the stress regime in the Aegean.

A simple stress model is shown in Fig. 12(b) to further clarify these effects. The fault system is driven by fixed displacements in the east and stresses are calculated for normal faults with the orientations shown. The change in strike of the fault in the Sea of Marmara region enhances normal faulting. Further to the southwest, the progressive reduction of slip causes normal faulting to be enhanced on the northwest side of the fault and suppressed on the southeast side. Fig. 12(a) shows that the increased activity of the Aegean grabens falls where increased activity is predicted by the model and activity is reduced on the other side (Armijo *et al.* 1996). The effect is also observed in the regional seismic activity, which is enhanced in the red region and suppressed in the blue (Fig. 12a). Similar features can be seen in GPS estimates of the strain field of the two regions (Khale *et al.* 1999, 2000).

Time varying stresses and displacements

The models described earlier are driven by displacement boundary conditions and evolve by the progressive addition of dislocation elements to represent dykes or faults. For such a system, stresses change as the system evolves. En echelon features in the Gulf of Aden result from stress rotation once the mantle fracture has formed and cannot be explained by a constant regional stress field. Similarly, shifting activity on the North Anatolian and East Anatolian faults result from stress fields. For both to move, the stress system must also evolve with time. If the lithosphere behaves in an elasto-plastic manner then the concept of a regional stress field is of limited value. In reality stresses and displacement rates on fault systems vary with time.

The effects of gravity

While gravity is not expected to have a significant effect on small-scale elasto-plastic deformation, at the scale of the Earth's lithosphere its effects become significant. For continents, although peaks and ridges can be higher, mountain plateaux do not rise more than 5 km above sea level and valley floors do not lie more than 2 km below sea level. Thin viscous sheet models of continental deformation specifically include the effects of gravity and seek to explain features of topography such as the Tibetan plateau (Houseman & England 1986, 1989).

Although we propose that the rheology of oceanic and continental lithosphere is similar, their response to the effects of gravity differ profoundly. Oceanic lithosphere is created at ocean ridges and is returned to the mantle at trenches. This is not true for the continental lithosphere; it is too buoyant. In Fig. 13(a), the upper mantle is extended by dyke intrusion. Magma rises from the asthenosphere (as for ocean ridges), but cannot create large quantities of buoyant crust. Thus a depression forms above the extending mantle. This topography creates stresses that resist further opening in the upper-mantle. The resistance depends on the depth of the valley although if the valley fills with sediment (or water), stresses resisting opening are reduced. If the valley can become sufficiently deep, magma can rise to form a spreading ridge and under these conditions new ocean floor will form. The Gulf of Aden and Red Sea provide examples of stretching that evolves into sea floor spreading. On the other hand, the forces can be sufficient to suppress opening so that continued motion must be accommodated by the creation of new mantle dykes with the locus of deformation shifting elsewhere; ocean floor is not created. The Aegean and the Basin and Range appear to have evolved in this way. Over long periods of time, deformation becomes distributed over a number of structures, but at any time activity is restricted to very few. Originally noted by Wallace (1984) for the Basin and Range and Armijo *et al.* (1996) for

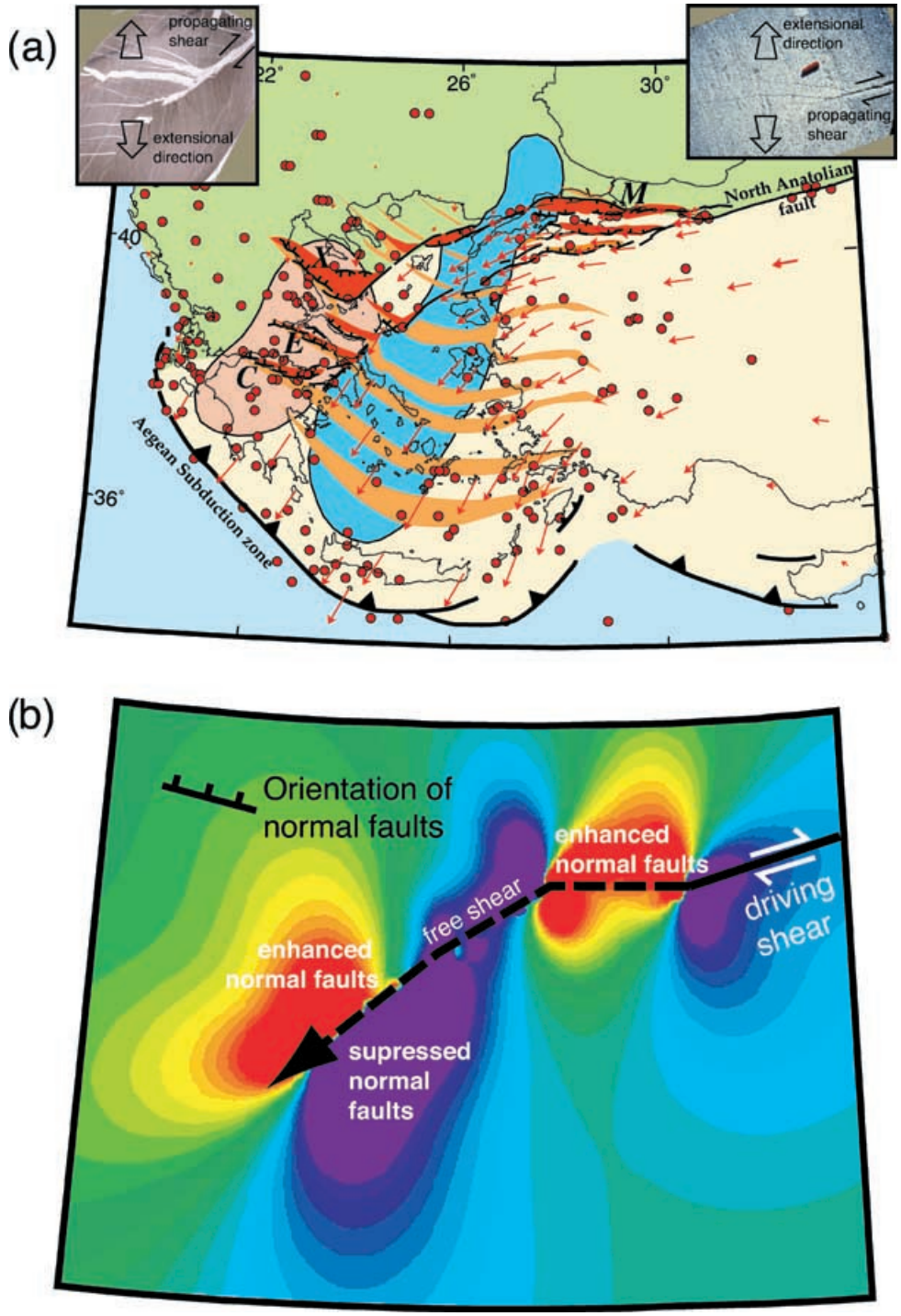

Figure 12. The propagation of the North Anatolian Fault (NAF) into the Aegean (a) Structures associated with Aegean extension (backarc extension due to subduction starting about 15 Ma) are shown schematically in orange. Red arrows are GPS vectors from McClusky *et al.* (2000). Red regions are extensional structures whose activity was increased by propagation of the NAF. Circles show earthquakes greater than magnitude 5 since 1965. Pink and blue regions indicate regions where the propagating NAF has increased and decreased activity on the normal faults as described in (b). Seismic activity is enhanced in the pink region and reduced in the blue region. Insets show small-scale field examples of shear faults propagating into regions with different extensional stress systems. In the right-hand figure, the extensional stress is nearly perpendicular to the propagating fault so that features sub-parallel to the fault are activated. Conditions when the NAF reached the future Sea of Marmara (*M* in the figure) are thought to have been similar. The left-hand inset shows a strike slip fault (with a small extensional component) reactivating structures at a high angle to the fault as a result of an extensional stress field at approximately 45° to the fault. This case is similar to the re-activation of the Gulfs of the western Aegean (*X*, *E* and *C* in the figure). (b) Coulomb stresses enhancing (red colours) and suppressing (mauve and blue colours) activity on normal faults with the strike indicated. The scale is taken to be the same as in (a), but the fault system is greatly simplified. The system is driven by fixed relative displacements on elements representing the NAF. Other elements are freely slipping. The fault geometry creates an extensional pull-apart in the Sea of Marmara region (*M*). In the Aegean, activity is increased in the west and reduced on the eastern side of the fault.

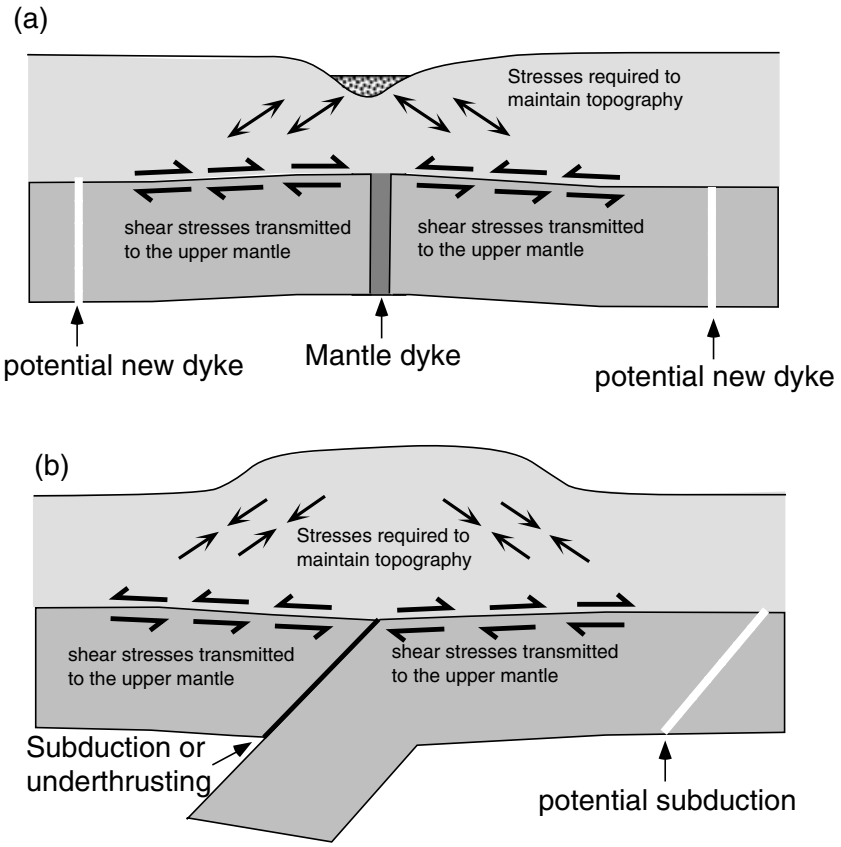

Figure 13. The effect of gravity on extensional and contractional boundaries in the continental lithosphere. (a) Extension in the upper mantle and lower crust is accommodated by the intrusion of dykes. In the upper crust all or part of the deformation must be accommodated by extensional faulting. This forms a depression which resists further opening. The magnitude of the stresses created by the topography depends on the depth of the surface depression (Molnar & Lyon-Caen 1988). If the depression becomes too deep (>3 km), new zones of extension can be created (dashed white lines). At any time only a single feature is active but the locus activity shifts over time. This produces a geological record of distributed deformation. Filling of the depression with sediment (or water) reduces the resultant stresses. Consequently localized extensional features can form more readily in oceans or lakes or where sedimentation is high. These features can also be re-activated after a period of quiescence when erosion and sedimentation have smoothed the topography. The presence of low-density magma that can rise in the upper crust also promotes extension. (b) Similar conditions exist for regions of contraction. Stresses resulting from the creation of topography resist further subduction of the upper mantle. Topographic relief in contractional regions (>5 km) is greater than in extensional regions. This probably reflects the greater forces required to create a new subduction zone (dashed white line) than to initiate new extension. Erosion of topography can also permit reactivation of older structures.

the Aegean, recent geodetic results (Thatcher *et al.* 1999; McClusky *et al.* 2000) have confirmed localisation of deformation for both regions.

Fig. 13(b) shows the equivalent mechanics for a compressional region. The upper mantle and possibly part of the lower crust can be faulted or subducted into the mantle while the upper crust thickens. Again forces maintaining topography resist continued thickening causing mantle subduction to shift elsewhere. The clearest examples are in Tibet (Tapponnier *et al.* 2001).

Unlike contraction or extension, continental crust does not resist strike-slip motion and such faults are consequently more long lived. However, triple junctions that result from the intersection of such boundaries are geometrically unstable (McKenzie & Morgan 1969) and must evolve with time (e.g. King 1983). This effect combined with the limited life of continental extension or subduction means that continental plates are ephemeral. Over long time periods this results in more widespread deformation of the continental lithosphere than oceanic lithosphere. Widespread deformation however, does not indicate a fundamental difference in rheology between oceanic and continental lithosphere.

CONCLUSIONS

The objective of this paper is to show that simple modifications of the concepts of fracture mechanics are appropriate for understanding the evolution of the continental lithosphere and that elastic models can be used to examine the kinematics of the propagation of major tectonic structures. The success of such modelling suggests that the lithosphere exhibits elasto-plastic (elasto-brittle) behaviour rather than elasto-viscous behaviour. Any viscous relaxation must, either be too limited in extent (e.g. postseismic viscous relaxation) to affect the gross behaviour of the lithosphere, or the relaxation time must be many 10 s of millions of years, much longer than the time scales associated with propagation.

The Gulf of Aden took 15 Ma to propagate from the Owen Fracture zone to Afar and follows a path readily explained as fracture in an elastic lithosphere. Small-scale en echelon features are explained by upward propagation of the lower lithospheric fracture that opens obliquely following its initial formation. Large scale offsets result from the interaction between the lower lithosphere fracture and pre-existing lithospheric structures parallel to the African coast.

The Anatolian faults are attributed to escape tectonics from the collision between Arabia and Eurasia. Modelling predicts that the East Anatolian Fault should form first. Stresses are not appropriate for the creation of the North Anatolian Fault until the East Anatolian Fault has formed. Once formed, the path that the North Anatolian Fault has followed into the Aegean is consistent with the calculated stresses. Slab pull may enhance the propagation of the North Anatolian Fault, but cannot explain its east to west propagation. The model suggests that the East Anatolian Fault and North Anatolian Fault should not be simultaneously active, but little information exists to determine the time period over which activity switches between them. Over historical time, however it is clear that the two faults are not simultaneously active. The effect of propagation modifying activity is also illustrated in the Aegean where pre-existing features, to the northwest of the propagating North Anatolian Fault, have been increased in activity while activity to the southeast has been suppressed. This effect is observed both in the present seismicity and geodesy.

Unlike small-scale features, large-scale continental structures can be affected by gravity. This has little effect on strike-slip faults but extensional or contractional regimes produce valleys or mountains at the surface because continental crust cannot be created or subducted respectively. To form this topography, work is done against gravity. As a result, stresses resist continued extension or contraction of the continental lithosphere. This appears to control differences between oceanic and continental tectonics. In the former ridges and trenches persist. For continents, only strike-slip faults are relatively long lived.

ACKNOWLEDGMENTS

The authors thank many people for discussions that resulted in this paper, although the responsibility for the content is entirely our own. Renata Dmowska and James Rice were most helpful in directing us to important literature in the field of fracture mechanics. A morning spent with Frank McClintock was particularly revealing concerning the limitations of the mathematical theories of plasticity. His remark that our data in Earth Science on the propagation of great faults and rifts is better than the data available to engineers was thought provoking. Many people have read and reviewed versions of the manuscript with David Bowman, Amotz Agnon and Shelley Kenner deserving particular thanks. In a general sense this paper has resulted from support from INSU in France under programs such as l'ACI Cat. Nat., and PNRN. The European Community's environment programme also deserves mention under the titles of FAUST and PRESAP. This is INSU contribution No 333 and IPGP contribution No 1884.

REFERENCES

Abelson, M. & Agnon, A., 1997. Mechanics of oblique spreading and ridge segmentation, *Earth planet Sci. Lett.,* **148,** 405–421.

Abelson, M. & Agnon, A., 2001. Hotspot activity and plume pulses recorded by the geometry of spreading axes, *Earth planet Sci. Lett.,* **189,** 31–47.

Agnon, A. & Eidelman, A., 1991. Lithospheric breakup in three dimensions; necking of a work-hardening plastic plate, *J. geophys. Res.,* **96,** 20 189–20 194.

Aktas, G. & Robertson, A.H.F., 1984. The Maden complex. Se Turkey: Evolution of a Neotethyan active margin, in *The Geological Evolution of Eastern Mediterranean,* Vol. 17, pp. 375–402, eds Dixon, J.E. & Robertson, A.H.F., Geological Society, London, Special Publication.

Ambraseys, N.N., 1970. Some characteristic features of the North Anatolian Fault zone, *Tectonophysics,* **9,** 143–165.

Ambraseys, N.N., 1971. Value of historical record of earthquakes, *Nature,* **232,** 375–379.

Ambraseys, N.N. & Melville, C.P., 1982. *A History of Persian earthquakes,* Cambridge University Press, Cambridge.

Ambraseys, N.N., 1989. Temporary seismic quiescence: SE Turkey, *Geophy. J. Int.,* **96,** 311–331.

Ambraseys, N.N. & Melville, C.P., 1995. Historical evidence of faulting in Eastern Anatolia and Northern Syria, *Annali di Geophysica,* **38,** 337–343.

Angelier, J., Lyberis, N., Le Pichon, X., Barrier, E. & Huchon, P., 1982. The tectonic development of the Hellenic arc and the Sea of Crete, a synthesis, *Tectonophysics,* **86,** 159–196.

Armijo, R., Lyon-Caen, H. & Papanastassiou, D., 1992. East-West extension and Holocene normal-fault scarps in the Hellenic arc, *Geology,* **20,** 491–494.

Armijo, R., Meyer, B., King, G.C.P., Rigo, A. & Papanastassiou, D., 1996. Quaternary Evolution of the Corinth Rift and its Implications for the Late Cenozoic Evolution of the Aegean, *Geophys, J. Int.,* **126,** 11–53.

Armijo, R., Meyer, B., Hubert-Ferrari, A. & Barka, A., 1999. Propagation of the North Anatolian Fault into the Northern Aegean: Timing and Kinematics, *Geology,* **27,** 267–270.

Armijo, R., Meyer, B., Navarro, S., King, G.C.P. & Barka, A., 2002. Asymmetric slip partitioning in the Sea of Marmara pull-apart: a clue to propagation processes of the North Anatolian Fault?, *TerraNova,* **14,** 80–86.

Audin, L., 1999. Pénétration de la dorsale d'Aden dans la dépression Afar entre 20 et 4 Ma, *PhD thesis,* Universite Paris VII, France.

Avigad, D., Baer, G. & Heimann, A., 1998. Block rotation and continental extension in the central Aegean Sea: paleomagnetic and structural evidence from Tinos and Mykonos, Cyclades, Greece, *Earth planet. Sci. Lett.,* **157,** 23–40.

Barka, A., Saroglu, F. & Güner, Y., 1983. 1983 Horasan-Narman depremi ve bu depremin Dogu Anadolu neotektonigindeki yeri, *Turkiye Jeoloji Kurumu,* **8,** 16–21.

Barka, A., Kuscu, I. & Katp, H., 1985. Horasan-Narman (Erzurum, Turkey) earthquake of the 30th october 1983, in *Research on Earthquake Faults, Active Faults and Earthquake Prediction,* pp. 70–83, Minist. Int. Trade and Ind., Agency Ind. Sci. and Technol., Tokyo, Japan.

Barka, A.A. & Kadinsky-Cade, K., 1988. Strike-slip fault geometry in Turkey and its influence on earthquake activity, *Tectonophysics,* **7,** 663–684.

Barka, A.A., 1996. Slip distribution along the North Anatolian Fault associated with the large earthquakes of the period 1939 to 1967, *Bull. seism. Soc. Am.,* **86,** 1238–1254.

Barka, A., Serdar, A.H., Cohen, H.A. & Watchorn, F., 2000. Tectonic evolution of the Niksar and Tasova-Erbaa pull-apart basins, North Anatolian Fault zone; their significance for the motion of the Anatolian Block, *Tectonophysics,* **322,** 243–264.

Barr, T.D. & Dahlen, F.A., 1989. Brittle frictional mountain building 2. Thermal structure and heat budget, *J. struc Geol.,* **94,** 3923–3947.

Bercovici, D., 1996. Plate generation in a simple model for lithosphere-mantle flow with dynamic lubrication, *Earth planet. Sci. Lett.,* **144,** 41–51.

Bilham, R. & King, G.C.P., 1989. The morphology of strike-slip faults: Examples from the San Andreas, California, *J. geophys. Res.,* **94,** 10 204–10 216.

Bird, P., 1991. Lateral extrusion of lower crust from under high topography, in the isostatic limit, *J. geophys. Res.,* **96,** 10 275–10 286.

Bowden, F.P. & Tabor, D., 1950. Friction and Lubrication of Solids Part I. Clarendon Press, Oxford.

Bowden, F.P. & Tabor, D., 1964. Friction and Lubrication of Solids Part II. Clarendon Press, Oxford.

Brace, W.F. & Kohlstedt, D.L., 1980. Limits on lithospheric stress imposed by laboratory experiments, *J. geophys. Res.,* **85,** 6248–625.

Braun, J., Chery, J., Poliakov, A., Mainprice, D., Vauchez, A., Tomassi, A. & Daignieres, M., 1999. A simple parameterization of strain localization in the ductile regime due to grainsize reduction: a case study for olivine, *J. geophys. Res.,* **104,** 25 167–25 181.

Briais, A., Patriat, P. & Tapponnier, P., 1993. Updated interpretation of magnetic anomalies and seafloor spreading stages in the South China Sea; implications for the Tertiary tectonics of Southeast Asia, *J. geophys. Res.,* **98,** 6299–6328.

Bürgmann, R., Pollard, D.D. & Martel, S.J., 1994. Slip distributions on faults: effects of stress gradients, inelastic deformation, heterogeneous host-rock stiffness, and fault interaction, *J. struct. Geol.,* **16,** 1675–1690.

Cianetti, S., Gasperini, P., Boccaletti, M. & Giunchi, C., 1997. Reproducing the velocity and stress fields in the Aegean region, *Geophys. Res. Lett.,* **24,** 2087–2090.

Cloetingh, S., Burov, E. & Poliakov, A., 1999. Lithosphere folding; primary response to compression?(from Central Asia to Paris Basin), *Tectonics,* **6,** 1064–1083.

Cochran, J.R., 1981. The Gulf of Aden: structure and evolution of a young oceanic basin and continental margin, *J. geophys. Res.,* **86,** 263–288.

Courtillot, V., Galdeano, A. & Le Mouel, J.P., 1980. Propagation of an accreting plate boundary: A discussion of new aeromagnetic data in the Gulf of Tadjurah and Southern Afar, *Earth planet. Sci. Lett.,* **47,** 144–160.

Cowie, P.A. & Scholz, C.H., 1992a. Physical explanation for the displacement-length relationship of faults using a post-yield fracture mechanics model, *J. struct. Geol.,* **14,** 1133–1148.

Cowie, P.A. & Scholz, C.H., 1992b. Growth of faults by accumulation of seismic slip, *J. geophys. Res.,* **97,** 11 085–11 095.

Crouch, S.L. & Starfield, A.M., 1983. Boundary element methods in solid mechanics, Allen & Unwin, Winchester, Mass.

Dawers, N.H., Anders, M.H. & Scholz, C.H., 1993. Growth of normal faults: displacement-length scaling, *Geology,* **21,** 1107–1110.

De Mets, C., Gordon, R.G., Argus, D.F. & Stein, S., 1990. Current plate motions, *Geophys. J. Int.,* **101,** 425.

Dewey, J.F., Hempton, M.R., Kidd, W.S.F., Saroglu, F. & Sengör, A.M.C., 1986. Shortening of continental lithosphere: the neotectonics of eastern Anatolia—A young collision Zone, in *Collision Tectonics, Special Publication 19,* 3–36, eds Coward, M.P. & Ries, A.C., Geological Society, London.

Ebinger, C.J., Yeman, T., Harding, D.J., Tesfaye, S., Kelley, S. & Rex, D.C., 2000. Rift deflection, migration, and propagation; linkage of the Ethiopian and Eastern rifts, Africa, *Geol. Soc. Amer. Bull.,* **112,** 163–176.

England, P. & Jackson, J., 1989. Active deformation of the continents, *Ann. Rev. Planet. Sci.,* **17,** 197–226.

England, P. & McKenzie, D., 1982. A thin viscous sheet model for continenetal deformation, *Geophys. J. R. astr. Soc.,* **70,** 295–321.

Erinc, S., 1953. *Dogu Anadolu'nun Cografyasi,* Istanbul University, Istanbul.

Eyidogan, H., 1988. Rates of crustal deformation in western Turkey as deduced from major earthquakes, *Tectonophysics,* **148,** 83–92.

Fantozzi, P.L., 1996. Transition from continental to oceanic rifting in the Gulf of Aden; structural evidence from field mapping in Somalia and Yemen, *Tectonophysics,* **259,** 285–311.

Garfunkel, Z., 1981. Internal structure of the Dead Sea leaky transform (rift) in relation to plate kinematics, *Tectonophysics,* **80,** 81–108.

Gomberg, J.S., 1993. Tectonic deformation in the New Madrid seismic zone; inferences from map view and cross-sectional boundary element models, *J. geophys. Res.,* **98,** 6639–6664.

Gupta, A. & Scholz, C., 1998. Utility of elastic models in predicting fault displacement fields, *J. geophys. Res.,* **103,** 823–834.

Hébert, H., Deplus, C., Huchon, P., Khanbari, K. & Audin, L., 2001. Lithospheric structure of a nascent spreading ridge inferred from gravity data: The western Gulf of Aden, *J. geophys. Res.,* **106,** 26 345–26 364.

Hempton, M.R., 1985. Structure and deformation history of the bitlis suture near lake Hazar, southern Turkey, *Geol. Soc. Amer. Bull.,* **96,** 233–243.

Houseman, G. & England, P., 1986. Finite strain calculations of continental deformation. 1. Method and general results for convergent zone, *J. geophys. Res.,* **91,** 3651–3663.

Houseman, G. & England, P., 1989. Extension during continental convergence with application to the Tibetan Plateau, *J. geophys. Res.,* **94,** 17 561–17 579.

Hubert-Ferrari, A., 1998. La faille Nord-Anatolienne (cinématique, morphologie, localisation, vitesse et décalage total) et modélisations utilisant la contrainte de Coulomb sur différentes échelles de temps, *PhD thesis,* University of Paris VII Denis Diderot, Paris.

Hubert-Ferrari, A., Barka, A., Jacques, E., Nalbant, S., Meyer, B., Armijo, R., Tapponnier, P. & King, G.C.P., 2000. Seismic hazard in the Sea of Marmara Following the Izmit Earthquake, *Nature,* **404,** 269–273.

Hubert-Ferrari, A., Armijo, R., King, G.C.P., Meyer, B. & Barka, A., 2002. Morphology, displacement and slip rates along the North Anatolian Fault (Turkey), *J. geophys. Res.,* **107,** B10, ETG9–1 to ETG9–33.

Joffe, S. & Garfunkel, Z., 1987. Plate kinematics of the circum Red Sea—a re-evaluation, *Tectonophysics,* **141,** 5–22.

Jolivet, L., Brun, J., Gautier, P., Lallemant, S. & Patriat, M., 1994. 3D kinematics of extension in the aegean region from early Miocene to the present, insights from the ductile crust, *Bull. Soc. Geol. Fr.,* **165,** 195–209.

Katzman, R., ten Brink, U.S. & Lin, J., 1995. 3-D modeling of pull-apart basins: Implications for the tectonics of the Dead Sea Basin, *J. geophys. Res.,* **100,** 6295–6312.

Kasapoglu, K. & Toksoz, M., 1983. Tectonic consequences of the collision of the Arabian and Eurasian Plates: finite element models, *Tectonophysics,* **100,** 71–95.

Ketin, I., 1969. About the strike-slip movenent of North Anatolia, *Bull. Miner. res. Explor. Inst. Turkey,* **72,** 1–28 (in German).

Khale, H.-G., Cocard, M., Peter, Y., Geiger, A., Reilinger, R., Barka, A. & Veis, G., 2000. GPS-derived strain rate field within the boundary zones of the Eurasian, African, and Arabian Plates, *J. geophys. Res.,* **105,** 23 353–23 370.

Khale, H.-G. *et al.*, 1999. GPS strain rate field in the Aegean Sea and the western Anatolia, *Geophys. Res. Lett.,* **26,** 2513–2516.

King, G.C.P., 1983. The accommodation of strain in the upper lithosphere of the earth by self-similar fault systems; the geometrical origin of b-value, *Pure appl. Geophys.,* **121,** 761–815.

King, G.C.P. & Sammis, C., 1991. The Mechanisms of Finite Brittle Strain, *Pageoph,* **138,** 611–640.

King, G.C.P. & Cocco, M., 2000. Fault interaction by elastic stress changes: new clues from earthquake sequences, *Advances in Geophysics, Academic Press,* **44,** 1–38.

Klein, A., Jacoby, W.R. & Smilde, P., 1997. Mining-induced crustal deformation in Northwest Germany; modelling the rheological structure of the lithosphere, *Earth planet. Sci. Lett.,* **147,** 107–123.

Knott, J.F., 1973. *Fundamentals of Fracture Mechanics,* Wiley, New-York.

Lawn, B.R. & Wilshaw, T.R., 1975. *Fracture of Brittle Solids,* Cambridge Univ. Press, Cambridge.

Leloup, P.H. *et al.*, 1995. The Ailao Shan-Red River shear zone (Yunnan, China), Tertiary transform boundary of IndochinaHilde, *Tectonophysics,* **251,** 3–84.

Lundgren, P., Giardini, D. & Russo, R., 1998. A geodynamic framework for eastern Mediterranean kinematics, *Geophys. Res. Lett.,* **25,** 4007–4010.

Lyakhovsky, V., 2001. Scaling of fracture length and distributed damage, *Geophys. J. Int.,* **144,** 114–122.

Lyberis, N., Yurur, T., Chorowicz, J., Kasapoglu E. & Gundogdu, N., 1992. The East Anatolian Fault: an oblique collisional belt, *Tectonophysics,* **204,** 1–15.

Lyon-Caen H. *et al.*, 1988. The 1986 Kalamata (South Peloponnesus) Earthquake: detailed study of a normal fault, evidences for East-West extension in the Hellenic arc, *J. geophys. Res.,* **93,** 14 967–15 000.

MacDonald, K.C., Scheirer, D.S. & Carbotte, S.M., 1991. Mid-ocean ridges; discontinuities, segments and giant cracks, *Science,* **253,** 986–994.

Manighetti, I., Tapponnier, P., Courtillot, V., Gruszow, S. & Gillot, P., 1997. Propagation of rifting along the Arabia-Somalia plate boundary: the Gulfs of Aden and Tadjoura, *J. geophys. Res.,* **102,** 2681–2710.

Martel, S.J., 1997. Effects of cohesive zones on small faults and implications for secondary fracturing and fault trace geometry, *J. Struct. Geol.,* **19,** 835–847.

Martel, S.J., 1999. Mechanical controls on fault geometry, *J. Struct. Geol.,* **21,** 585–596.

Martinod, J., Hatzfeld, D., Brun, J.P., Davy, P. & Gautier P., 2000. Continental collision, gravity spreading, and kinematics of Aegea and Anatolia, *Tectonics,* **19,** 290–299.

McClintock, F.A., 1971. Plasticity Aspects of Fracture, in *Fracture. An Advanced Treatise, Vol. III, Engineering fundamentals and Environment Effects*, ed. Liebowitz, H., Academic Press, New York.

McClusky, S. *et al.*, 2000. GPS constraints on plate motion and deformation in the eastern Mediteranean: Implication for plate dynamics, *J. geophys. Res.,* **105,** 5695–5719.

McKenzie, D.P. & Morgan, W.J., 1969. Evolution of triple junctions, *Nature,* **224,** 125–133.

McKenzie, D.P., 1972. Active tectonics of the Mediterranean region, *Geophys. J. R. astr. Soc.,* **30,** 109–185.

McKenzie, D.P., 1976. The East Anatolian Fault: A major structure in eastern Turkey, *Earth planet. Sci. Lett.,* **29,** 189–193.

Meijer, P. & Wortel, M., 1996. Temporal variation in the stress field of the Aegean region, *Geophys. Res. Lett.,* **23,** 439–442.

Meijer, P. & Wortel, M., 1997. Present-day dynamics of the Aegean region: a model analysis of the horizontal pattern of stress and deformation, *Tectonics,* **16,** 879–895.

Mercier, J.L., Sorel, D. & Vergely, P., 1989. Extensional tectonics regimes in the Aegean basins during the Cenozoic, *Basin Res.,* **2,** 49–71.

Meriaux, C., Lister, J.R., Lyakhovsky, V. & Agnon, A., 1999. Dyke propagation with distributed damage of the host rock, *Earth planet. Sci. Lett.,* **165,** 177–185.

Meyer, B., Tapponnier, P., Bourjot, L., Métivier, F., Gaudemer, Y., Peltzer, G., Guo Shunmin. & Chen Zhitai, 1998. Crustal thickening in Gansu-Qinghai, lithospheric mantle subduction and oblique, strike-slip controlled growth of the Tibetan Plateau, *Geophys. J. Int.,* **135,** 1–47.

Michard, A., Whitechurch, H. Ricou, L.E., Montigny, R. & Yazgan, E., 1984. Tauric subduction (Malatya-Elazig provinces) and its bearing on tectonics of the Tethyan realm in Turkey, in *The Geological Evolution of the Eastern Mediterranean,* Vol. 17, pp. 362–373, eds Dixon, J.E. & Robertson, A.H.F., Geological Society, London, Special Publication.

Molnar, P. & Lyon-Caen, H., 1988. Some simple physical aspects of the support, structure, and evolution of mountain belts, *Geol. Soc. Am. Spec. Paper,* **218,** 179–207.

Molnar, P. & England, P., 1990. Temperatures, heat flux, and frictional stress near major thrust faults, *J. geophys. Res.,* **95,** 4833–4856.

Morgan, J.P. & Parmentier, E.M., 1985. Causes and rate-limiting mechanisms of ridge propagation; a fracture mechanics model, *J. geophys. Res.,* **90,** 8603–8612.

Muehlberger, W.R. & Gordon, M.B., 1987. observation on the complexity of the east Anatolian Fault, Turkey, *J. Struct. Geol.,* **9,** 899–903.

Murphy, M.A., Yin, A., Kapp, P., Harrison, T.M., Ding Lin & Guo Jinghui, 2000. Southward propagation of the Karakoram fault system, Southwest Tibet; timing and magnitude of slip, *Geology,* **28,** 451–454.

Naborro, F.R.N., 1967. *Theory of crystal dislocations,* Clarendon Press, Oxford.

Nicolas, A., Bouchez, J.L., Blaise, J. & Poirier, J.P., 1977. Geological aspects of deformation in continental shear zones, *Tectonophysics,* **42,** 55–73.

Papazachos, C.B., 1999. Seismological and GPS evidence for the Aegean-Anatolia interaction, *Geophys. Res. Lett.,* **26,** 2653–2656.

Pearce, J.A. *et al.*, 1990. Genesis of collision volcanism in Eastern Anatolia, Turkey, *J. Volc. Geotherm. Res.,* **44,** 189–229.

Peacock, D.C.P. & Sanderson, D.J., 1996. Effects of propagation rate on displacement variations along faults, *J. Struct. Geol.,* **18,** 311–320.

Peltzer, G., Tapponnier, P. & Cobbold, P., 1982. Les grands décrochements de l'Est asiatique, évolution dans le temps et comparaison avec un modèle expérimental, *C.r. Acad. Sci. Paris,* **294,** 1341–1348.

Peltzer, G. & Tapponnier, P., 1988. Formation and evolution of strike-slip fauls, rift, and basins during the India-Asia collision: an experimental approach, *J. geophys. Res.,* 15 085–15 117.

Peltzer, G. & Saucier, F., 1996. Present-day kinematics of Asia derived from geological fault rates, *J. geophys. Res.,* **101,** 27 943–27 956.

Pili, E., Ricard, Y., Lardeaux, J.-M. & Sheppard, S.M.F., 1997a. Lithospheric shear zones and mantle-crust connections, *Tectonophysics,* **280,** 15–29.

Pili, E., Sheppard, S.M.F., Lardeaux, J.-M., Martelat, J.-E. & Nicollet, C., 1997b. Fluid flows vs. scale of shear zones in the lower continental crust and the granulite paradox, *Geology,* **25,** 15–18.

Poirier, J.P., 1980. Shear localization and shear instability in materials in the ductile field, *J. Struct. Geol.,* **2,** 135–142.

Reilinger, R.E. *et al.*, 1997. Global Positioning system measurements of the present-day crustal movements in the Arabia-Africa-Eurasia plate collision zone, *J. geophys. Res.,* **102,** 9983–9999.

Rudnicki, J.W., 1980. Fracture mechanics applied to the Earth's Crust, *Ann. Rev. Earth planet. Sci.,* **8,** 489–525.

Rundle, J.B. & Klein, W., 1989. Nonclassical nucleation and growth of cohesive tensile cracks,*Phys. Rev. Lett.,* **63,** 171–174.

Saroglu, F. & Guner, Y., 1981. Dogu Anadolunun jeomorfolojik gelisimine etki eden ögeler; jeomorfoloji, tektonik and volkanizma iliskileri, *Türkiye Jeol. Kur. Bült,* **24,** 269–282.

Saroglu, F., Emre, O. & Kuscu, I., 1988. The east Anatolian Fault zone of Turkey, Annales Tectonicae, *Sp. Issue,* **6,** 99–125.

Schindler, C., 1998. in *Geology of NW Turkey: results of the Marmara polyproject, dans Active Tectonics of Northwestern Anatolia—The Marmara Poly-Project, a multidisciplinary approach by space-geodesy, geology, hydrology, geothermics and seismology,* eds Schindler, C. & Pfister, M., Verlag der Fachvereine, Zurich.

Scholz, C.H., 1980. Shear heating and the state of stress on faults, *J. geophys. Res.,* **85,** 6174–6184.

Scholz, C.H., Dawers, N.H., YU, J.-Z., Anders, M.H. & Cowie, P.A., 1993. Fault growth and fault scaling laws: preliminary results, *J. geophys. Res.,* **98,** 21 951–21 961.

Sengör, A.M.C. & Kidd, W.S.F., 1979. Post-collisional tectonics of the Turkish-Iranian plateau and a comparaison with Tibet, *Tectonophysics,* **55,** 361–376.

Sengor, A.M.C., Gorur, N. & Saroglu, F., 1985. Strike-slip faulting and related basin formation in zones of tectonic escape: Turkey as a case study, in *Strike-slip faulting and Basin formation,* pp. 227–267, eds Biddle, K.T. & Christie-Blick N., Soc. Econ. Paleont. Min. Sp. Publ.

Seyitoglu, G., Scott, B.C. & Rundle, C.C., 1992. Timing of the Cenozoic extensional tectonics in western Turkey, *J. Geol. Soc. Lond.,* **149,** 533–538.

Tackley, P.J., 1998. Self-consistent generation of tectonic plates in three-dimensional mantle convection, *Earth planet. Sci. Lett.,* **157,** 9–22.

Tapponnier, P., Peltzer, G., Le Dain, A.Y., Armijo, A. & Cobbold, P., 1982. Propagating extrusion tectonics in Asia: new insights from simple experiments with plasticine, *Geology,* **10,** 611–616.

Tapponnier, P., Xu Zhiqin, Roger, F., Meyer, B., Arnaud, N., Wittlinger, G. & Yang Jingsui., 2001. Oblique, Stepwise Rise and Growth of the Tibetan Plateau, *Science,* **294,** 1671–1673.

Ten Brink, U.S., Katzman, R. & Lin. J., 1996. Three-dimensional models of crustal deformation near strike-slip faults, *J. geophys., Res.,*v. **101,** 16 205–16 220.

Thatcher, W., Foulger, G.R., Julian, B.R., Svarc, J., Quilty, E. & Bawden, G.W., 1999. Present day deformation across the Basin and Range Province, Western United States, *Science,* **283,** 1714–1718.

Tisseau, J., 1978. Etude structurale du Golfe d'Aden et du bassin de Somalie (Ocean Indien Occidental nord), *PhD thesis,* Univ. of Paris-sud, Paris XI.

Vilotte, J.P., Daigniere, M. & Madariaga, R., 1982. Numerical modelling of intraplate deformation: simple mechanical models of continental collision, *J. geophys. Res.,* **87,** 10 709–10 728.

Wallace, R.E., 1984. Patterns and Timing of Late Quaternary Faulting in the Great Basin Province and relation to some Regional tectonic features, *J. geophys. Res.,* **89,** 5763–5769.

Westaway, R., 1994. Present-day kinematics of the Middle East and eastern Mediterranean, *J. geophys. Res.,* **99,** 12 071–12 090.

Westaway, R. & Aeger, J., 1996. The Gölbasi basin, Southern Turkey: a complex discontinuity in a major strike-slip fault zone, *J. geol. Soc. Lond.,* **153,** 729–744.

Wright, T., Parsons, B. & Fielding, E., 2001. Measurement of interseismic strain accumulation across the North Anatolian Fault by satellite radar interferometry, *Geophys. Res. Lett.,* **28,** 2117–2120.

Yilmaz, Y., Saroglu, F. & Güner, Y., 1987. Initiation of the neomagnatism in East Anatolia, *Tectonophysics,* **134,** 177–199.

APPENDIX A: THE COULOMB CRITERIA

Whatever the detailed processes may be, a Coulomb Law is a reasonable first approximation to failure processes in a damage zone. The Coulomb Failure stress is defined as

$$\sigma_\phi = \tau - \mu' \sigma_n \tag{A1}$$

where σ_n and τ are the effective normal stress and shear stress acting on a plane and μ' is the effective friction coefficient. This expression allows the maximum Coulomb stresses and the plane of failure to be calculated and plotted (e.g. King & Cocco 2000). Alternatively, the Coulomb stress can be computed on pre-existing planes (defects) that may not optimally oriented. In this formulation, shear stress is always important while confining pressure may, or may not be, depending on the value of effective friction.

The choice of μ' is not straightforward. Values for the seismogenic crust between 0.1 and 0.8 have been proposed, but no values have been suggested for the deep lithosphere. At the latter depths, the deformation process is best described as elasto-plastic in which case μ' will probably be low. In the absence of better information we have used a value of 0.4. Critical regions of our models are only mildly sensitive to this choice (King & Cocco 2000).

APPENDIX B: PARAMETERS USED TO MODEL THE PROPAGATION OF THE ADEN RIDGE AND THE ANATOLIAN FAULTS

The Aden Ridge

The boundary conditions employed to model the creation and propagation of the Aden ridge are shown in Fig. B1. Manighetti *et al.* (1997) proposed a more simple geometry (inset top left) to explain the location and creation of the Gulf of Aden. They suggest that fracture occurred at the narrowest part of the previously continuous Arabian-Somali plate as a result of slab pull in the Zagros. In their simple model, fracture start at both sides and propagates directly to the center. The model that we propose has a more realistic geometry that correctly approximates the true positions of the plate boundaries. The positions were taken from the topographic map of Fig. 1, which has a conical projection that preserves the angular relations between the different plate boundaries. Slight errors are introduced because the modelling is planar and not on a sphere. The system is driven by displacements, relative to Somalia, specified on the Arabian plate side of the Zagros (elements 8–11). Elements 6 (Southern Dead Sea fault) and 12 (Southern Owen Fracture zone) are constrained such that slip is parallel to the plate boundary. These are locations where the direction of motion is well defined. It is possible to specify slip at other locations, but the boundary element calculation creates the values that are not specified. We choose to define other boundaries as stress free. To test that the system is properly constrained, free elements are introduced along the Aden ridge. This gives the set of slip vectors shown in the upper right inset. They are consistent with the Arabian-Somalia pole of rotation in the Gulf of Aden region. This provides confirmation that the chosen boundary conditions are appropriate. The model is insensitive to the presence the East Anatolian Fault which is not introduced in the model.

The Anatolian Fault Systems

The boundary conditions employed to model the creation and propagation of the Anatolian Fault systems are shown in Fig. B2. The positions of boundary elements were taken from the topographic map of Fig. 1, which has a conical projection that preserves the angular relations between the different plate boundaries. The boundary conditions are specified with respect to Eurasia by holding the southern side of element 1 fixed. It is also necessary to fix the normal displacement on the eastern side of element 2. This represents the transition to compression and mountain building in NW Greece and Albania. Elements 3 to 6 are stress free and can freely slip in any direction. In later models, to model slab pull a modest outward (normal) displacement of 0.25 along the subduction zone is introduced for elements 3 to 5. Elements 7–12 are free slipping strike-slip faults introduced progressively as discussed in the text. Elements 13–17 are free. In practice the model is insensitive to the presence or absence of elements 15–18 (dashed elements). The motion of Arabia to Eurasia is specified on the southern side of elements 18 and 19. To create a model with slip vectors, a temporary free element connects element 12 to the intersection of elements 2 and 3. The slip vectors are shown in the inset. The displacement vectors are consistent with those observed between Arabia and Eurasia in Anatolia. They differ from those in Fig. B2 which shows vectors relative to Somalia.

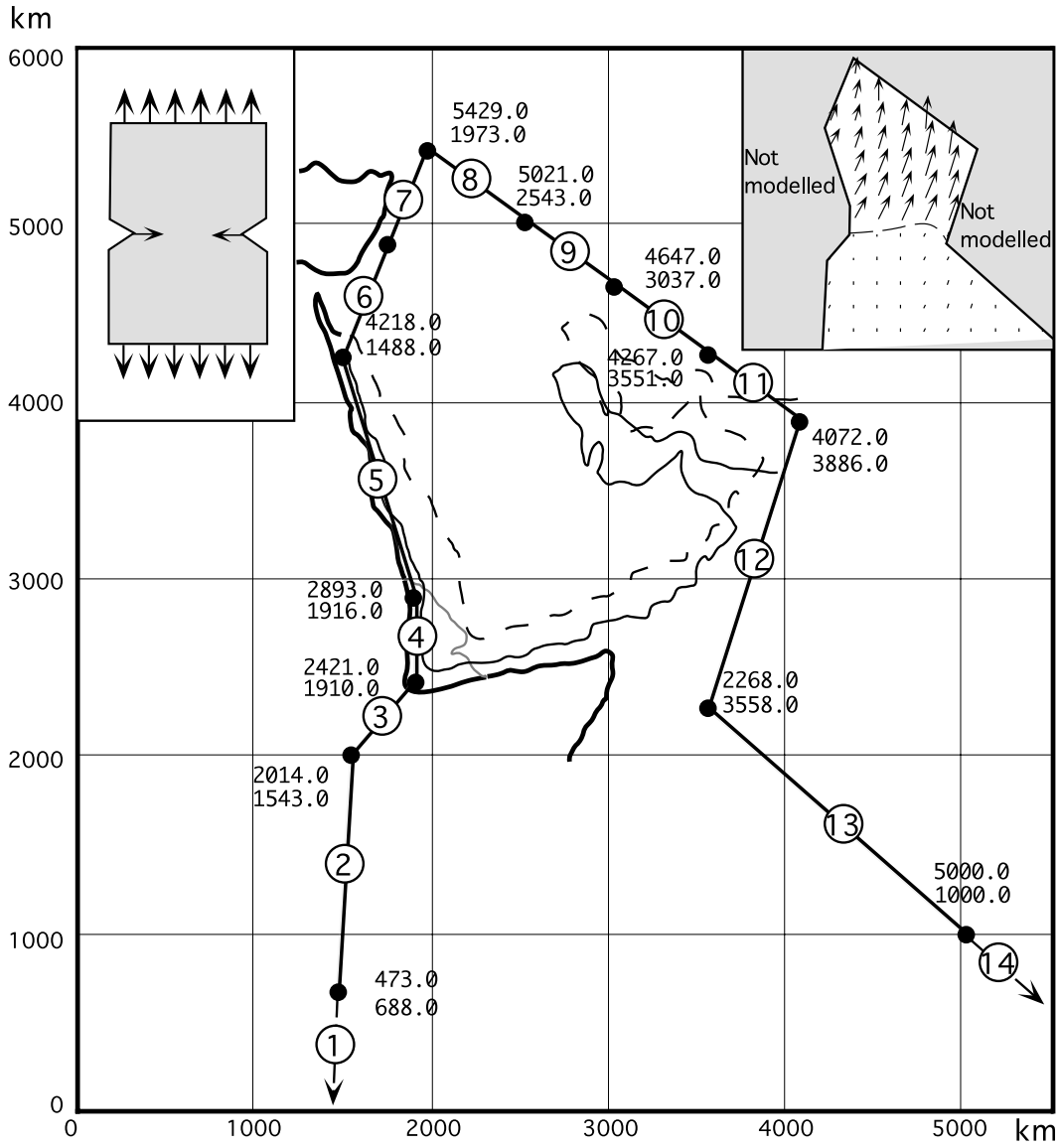

element	normal conditions		tangential conditions		remarks
	displacement	stress	displacement	stress	
1	free	0	free	0	free boundary
2	free	0	free	0	free boundary
3	free	0	free	0	free boundary
4	free	0	free	0	free boundary
5	free	0	free	0	free boundary
6	0 (relative)	free	free	0	free strike-slip
7	free	0	free	0	free boundary
8	1.5	free	1.0	free	Arabian-Somali plate motion
9	1.25	free	0.8	free	Arabian-Somali plate motion
10	1.0	free	0.6	free	Arabian-Somali plate motion
11	free	0	free	0	free boundary
12	0 (relative)	free	free	0	free strike-slip
13	free	0	free	0	free boundary
14	free	0	free	0	free boundary

Figure B1. The location and boundary conditions of boundary elements (table) used to model the evolution of the Gulf of Aden. The inset (top left) shows the simplified fracture concept suggested by Manighetti *et al.* (1997). Our modelling introduces more realistic loading which effects the direction and path of rupture. Pre-existing defects also affect the propagation (see text). The inset (top right) shows the slip vectors for the Arabian plate relative to Somalia once the Aden ridge has been created.

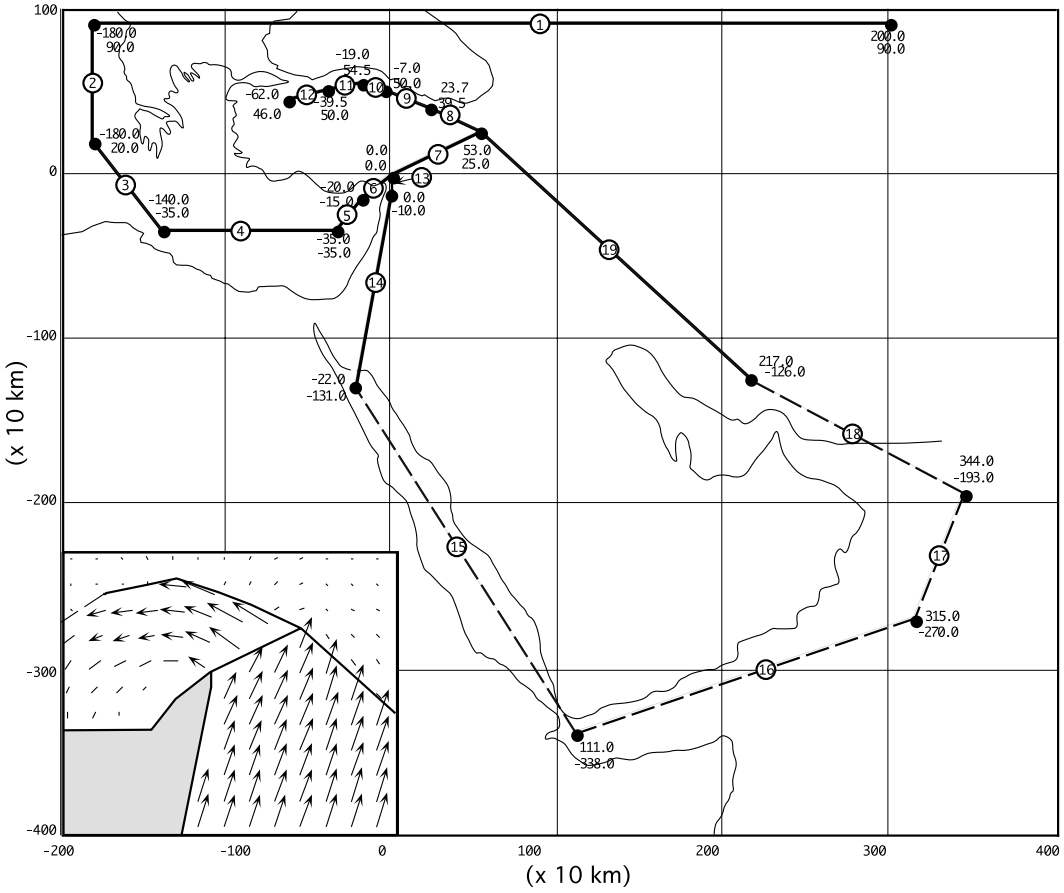

element	normal condx		tangential condx		remarks
	displacement	stress	displacement	stress	
1	0	free	free	0	Black Sea side fixed
2	0	free	free	0	Greek side fixed
3	free	0	free	0	free boundary
4	free	0	free	0	free boundary
5	free	0	free	0	free boundary
6	free	0	free	0	free boundary
7	0 (relative)	free	free	0	free strike-slip
8	0 (relative)	free	free	0	free strike-slip
9	0 (relative)	free	free	0	free strike-slip
10	0 (relative)	free	free	0	free strike-slip
11	0 (relative)	free	free	0	free strike-slip
12	0 (relative)	free	free	0	free strike-slip
13	free	0	free	0	free boundary
14	free	0	free	0	free boundary
15	free	0	free	0	free boundary
16	free	0	free	0	free boundary
17	free	0	free	0	free boundary
18	2.5	0	0.8	0	Arabia-Asia plate motion
19	2.5	0	0.8	0	Arabia-Asia plate motion

Figure B2. The location and boundary conditions of boundary elements (table) used to model the evolution of the Anatolian Fault System. The inset (bottom left) shows slip vectors relative to Eurasia.